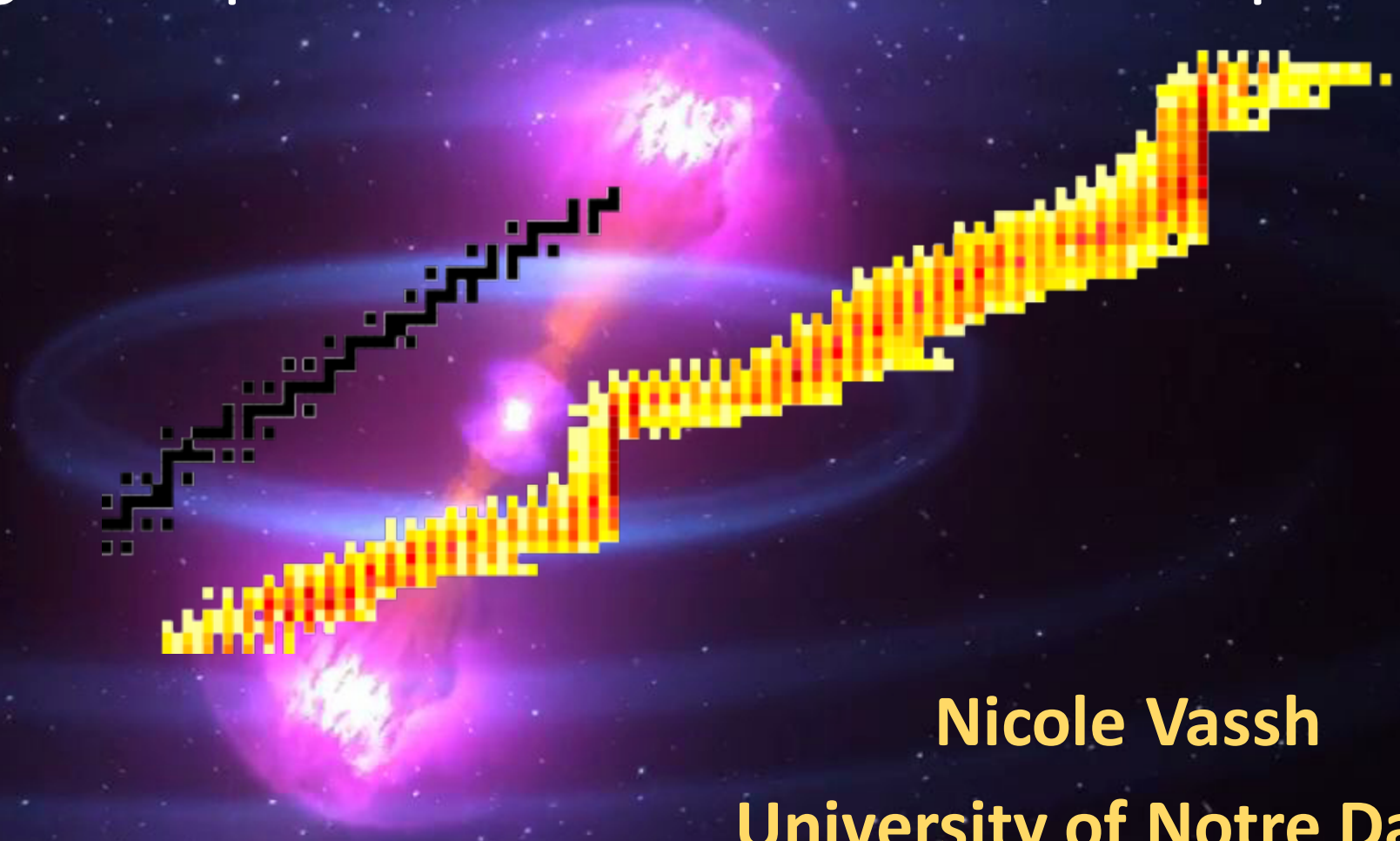


Reverse engineering properties of neutron-rich lanthanides by examining the *r*-process rare-earth abundance peak



Nicole Vassh

University of Notre Dame

INT-JINA Symposium 3/14/18

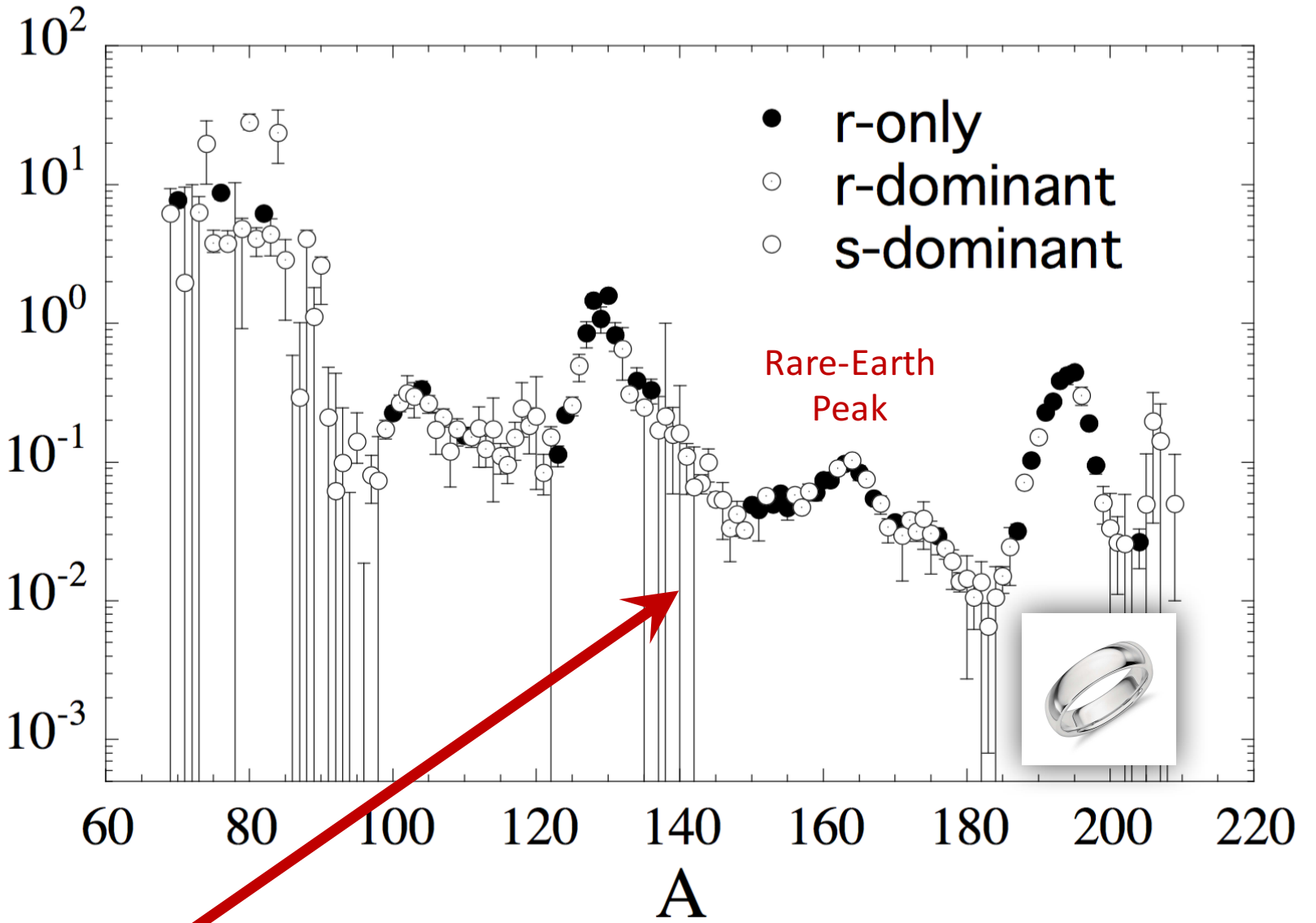


Fission In R-process
Elements



Observed Solar *r*-process Residuals

r-abundances [Si=10⁶]



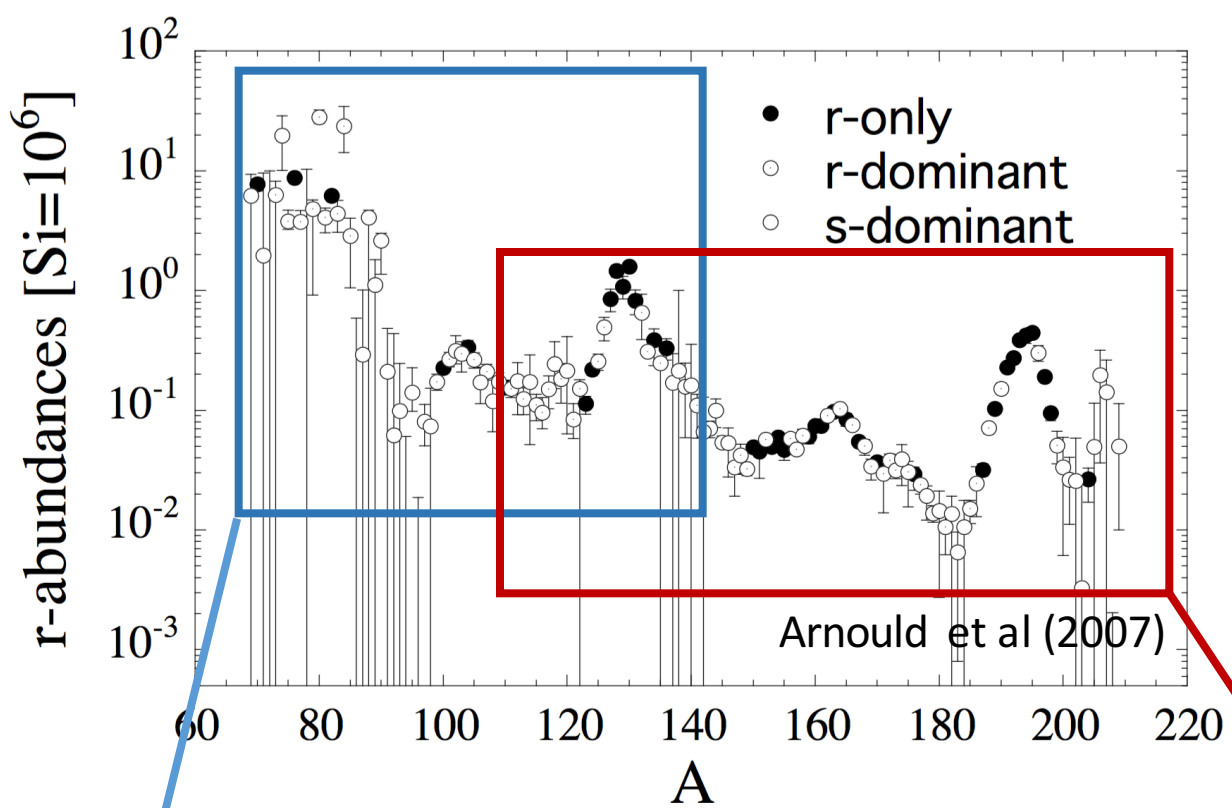
Arnould, Goriely and Takahashi (2007)

1 H Hydrogen 1.00794																	2 He Helium 4.003
3 Li Lithium 6.941	4 Be Beryllium 9.012182																
11 Na Sodium 22.989770	12 Mg Magnesium 24.3050																
19 K Potassium 39.0983	20 Ca Calcium 40.078	21 Sc Scandium 44.955910	22 Ti Titanium 47.887	23 V Vanadium 50.9415	24 Cr Chromium 51.9961	25 Mn Manganese 54.938045	26 Fe Iron 55.845	27 Co Cobalt 58.933200	28 Ni Nickel 58.6934	29 Cu Copper 63.546	30 Zn Zinc 65.39	31 Ga Gallium 69.723	32 Ge Germanium 72.61	33 As Arsenic 74.92160	34 Se Selenium 78.96	35 Br Bromine 79.904	36 Kr Krypton 83.80
37 Rb Rubidium 85.4678	38 Sr Strontium 87.62	39 Y Yttrium 88.90585	40 Zr Zirconium 91.224	41 Nb Niobium 92.90638	42 Mo Molybdenum 95.94	43 Tc Technetium (98)	44 Ru Ruthenium 101.07	45 Rh Rhodium 101.06550	46 Pd Palladium 106.42	47 Ag Silver 107.8682	48 Cd Cadmium 112.411	49 In Indium 114.818	50 Sn Tin 118.710	51 Sb Antimony 121.760	52 Te Tellurium 127.60	53 I Iodine 126.90447	54 Xe Xenon 131.29
55 Cs Cesium 132.90545	56 Ba Barium 137.327	57 La Lanthanum 138.905	58 Ce Cerium 140.90765	59 Pr Praseodymium 140.90765	60 Nd Neodymium 144.24	61 Pm Promethium (145)	62 Sm Samarium 150.36	63 Eu Europium 151.964	64 Gd Gadolinium 157.25	65 Tb Terbium 158.92534	66 Dy Dysprosium 162.50	67 Ho Holmium 164.93032	68 Er Erbium 167.26	69 Tm Thulium 168.93421	70 Yb Ytterbium 173.04	71 Lu Lutetium 174.967	
87 Fr Francium (223)	88 Ra Radium (226)	89 Ac Actinium (227)	90 Th Thorium 232.0381	91 Pa Protactinium 231.03688	92 U Uranium 238.0289	93 Np Neptunium (237)	94 Pu Plutonium (244)	95 Am Americium (243)	96 Cm Curium (247)	97 Bk Berkelium (247)	98 Cf Californium (251)	99 Es Einsteinium (252)	100 Fm Fermium (257)	101 Md Mendelevium (258)	102 No Nobelium (259)	103 Lr Lawrencium (262)	

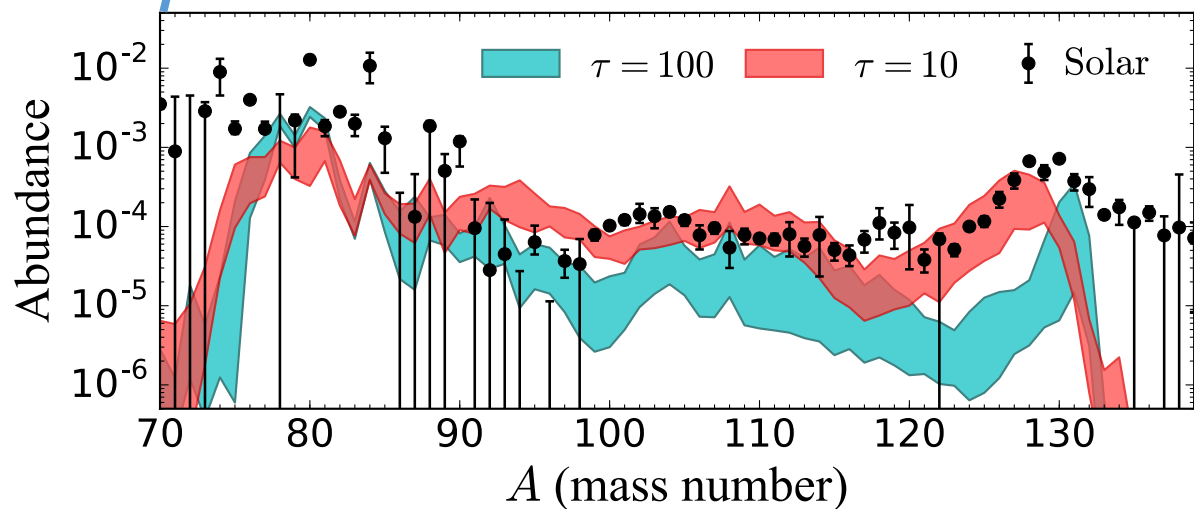
58 Ce Cerium 140.116	59 Pr Praseodymium 140.90765	60 Nd Neodymium 144.24	61 Pm Promethium (145)	62 Sm Samarium 150.36	63 Eu Europium 151.964	64 Gd Gadolinium 157.25	65 Tb Terbium 158.92534	66 Dy Dysprosium 162.50	67 Ho Holmium 164.93032	68 Er Erbium 167.26	69 Tm Thulium 168.93421	70 Yb Ytterbium 173.04	71 Lu Lutetium 174.967
90 Th Thorium 232.0381	91 Pa Protactinium 231.03688	92 U Uranium 238.0289	93 Np Neptunium (237)	94 Pu Plutonium (244)	95 Am Americium (243)	96 Cm Curium (247)	97 Bk Berkelium (247)	98 Cf Californium (251)	99 Es Einsteinium (252)	100 Fm Fermium (257)	101 Md Mendelevium (258)	102 No Nobelium (259)	103 Lr Lawrencium (262)

r-process Calculations for NSM Ejecta

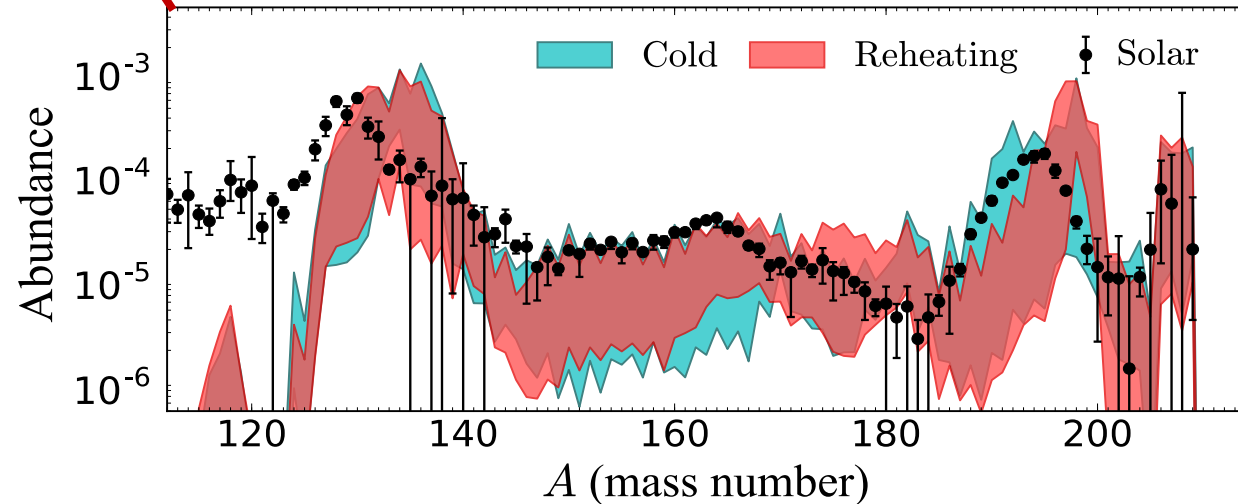
Côté, Fryer, Belczynski, Korobkin, Chruślińska, Vassh, Mumpower, Lippuner, Sprouse, Surman and Wollaeger (2017)



Wind ejecta ($s/k=10$, $Y_e=0.27$)

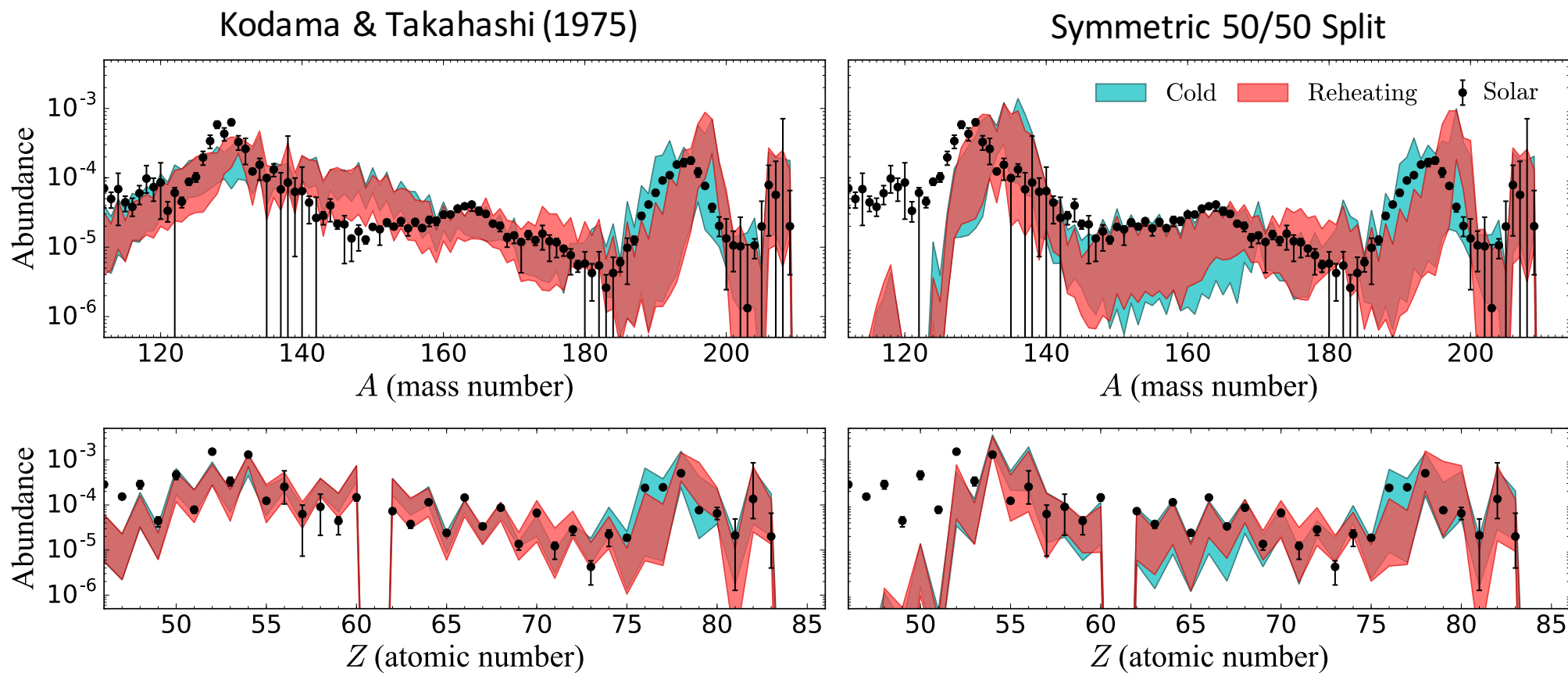


Very n-rich dynamical ejecta

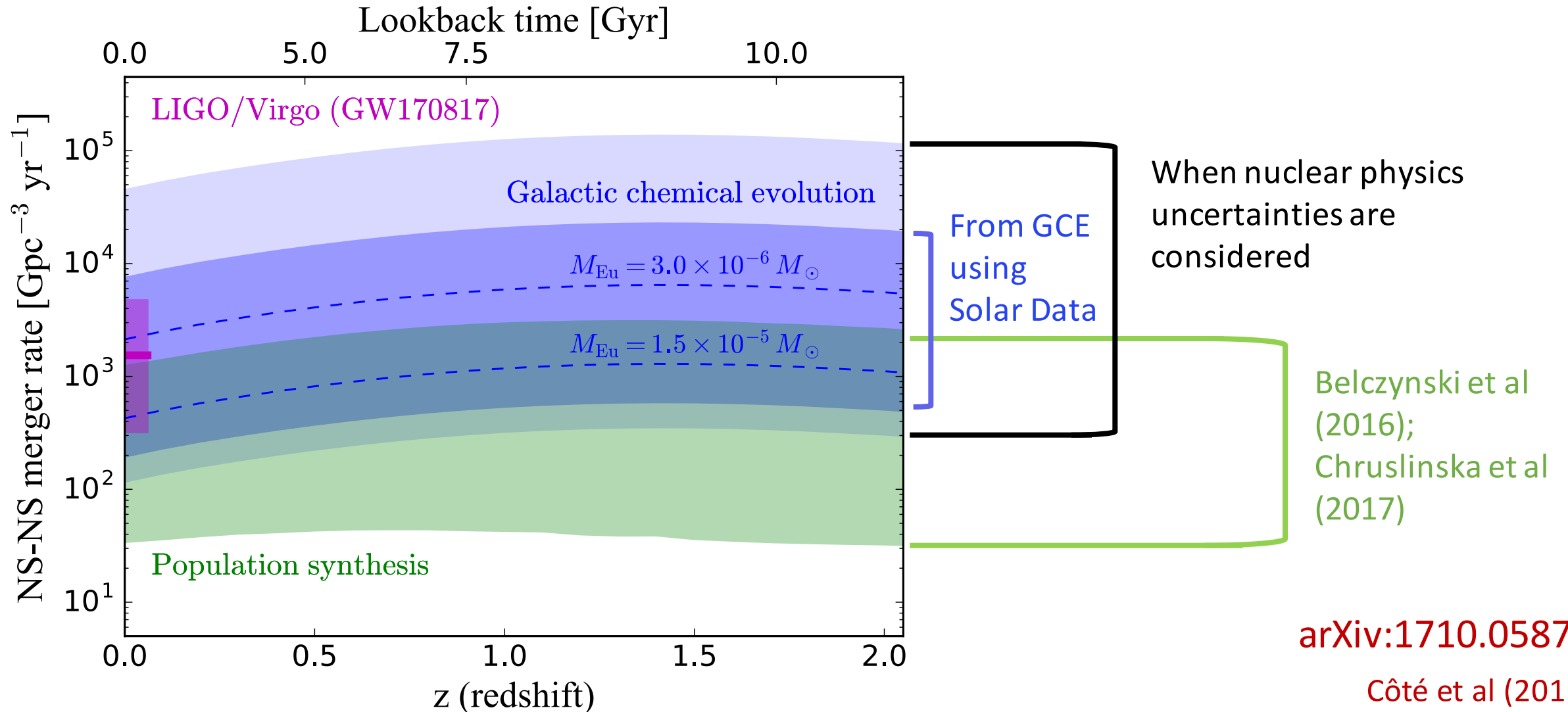


r -process Sensitivity to Mass Model and Fission Yields

- 10 mass models: DZ33, FRDM95, FRDM12, WS3, KTUY, HFB17, HFB21, HFB24, SLY4, UNEDF0
- N-rich dynamical ejecta conditions: **Cold** (Just 2015), **Reheating** (Mendoza-Temis 2015)



GW170817 and r -process uncertainties from nuclear physics



arXiv:1710.05875

Côté et al (2017)

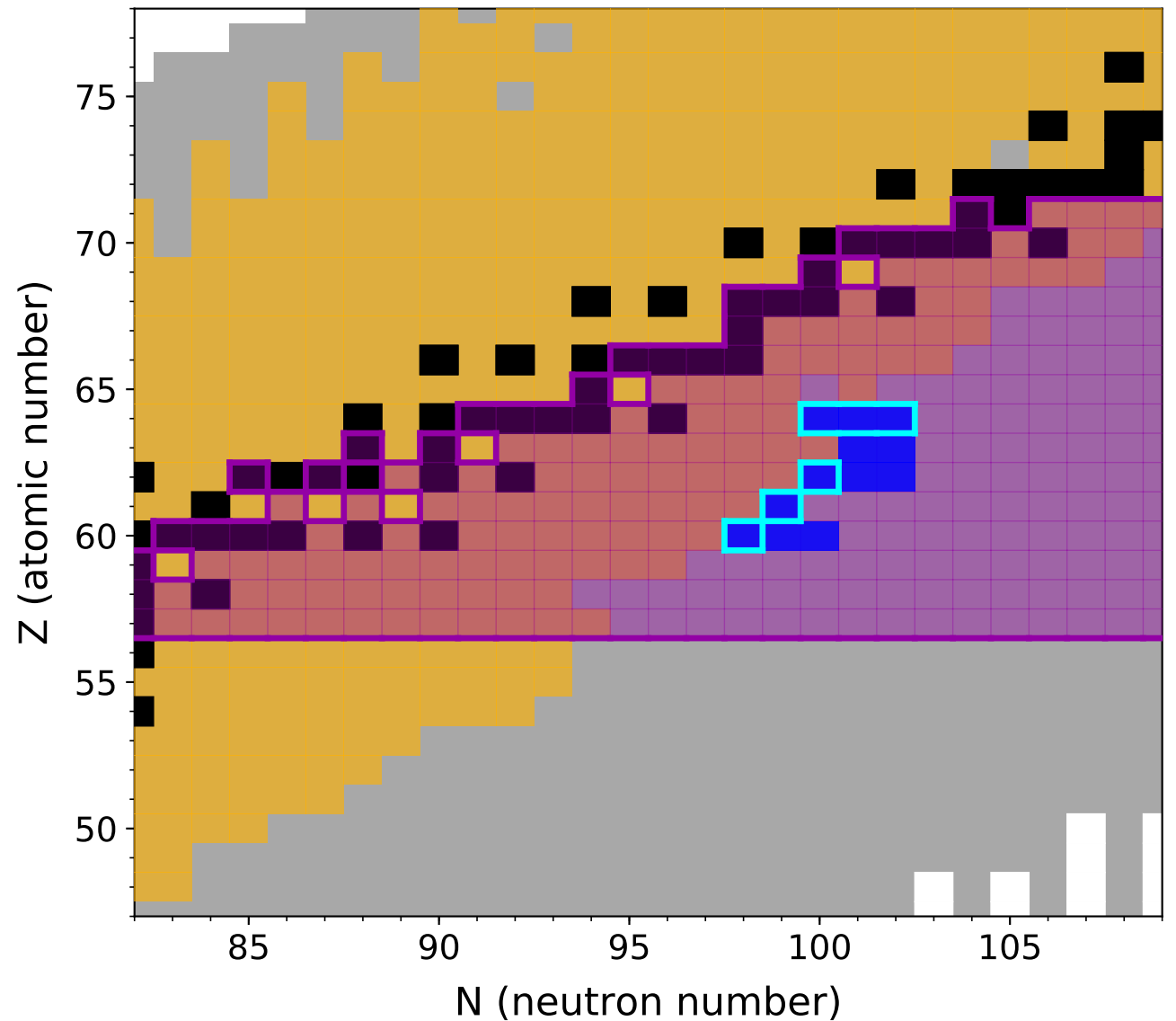
Studying Rare-Earth Nuclei to Understand *r*-process Lanthanide Production

Experimental Mass Measurements:

AME 2016

Jyväskylä

CPT at CARIBU



Studying Rare-Earth Nuclei to Understand *r*-process Lanthanide Production

Experimental Mass Measurements:

AME 2016

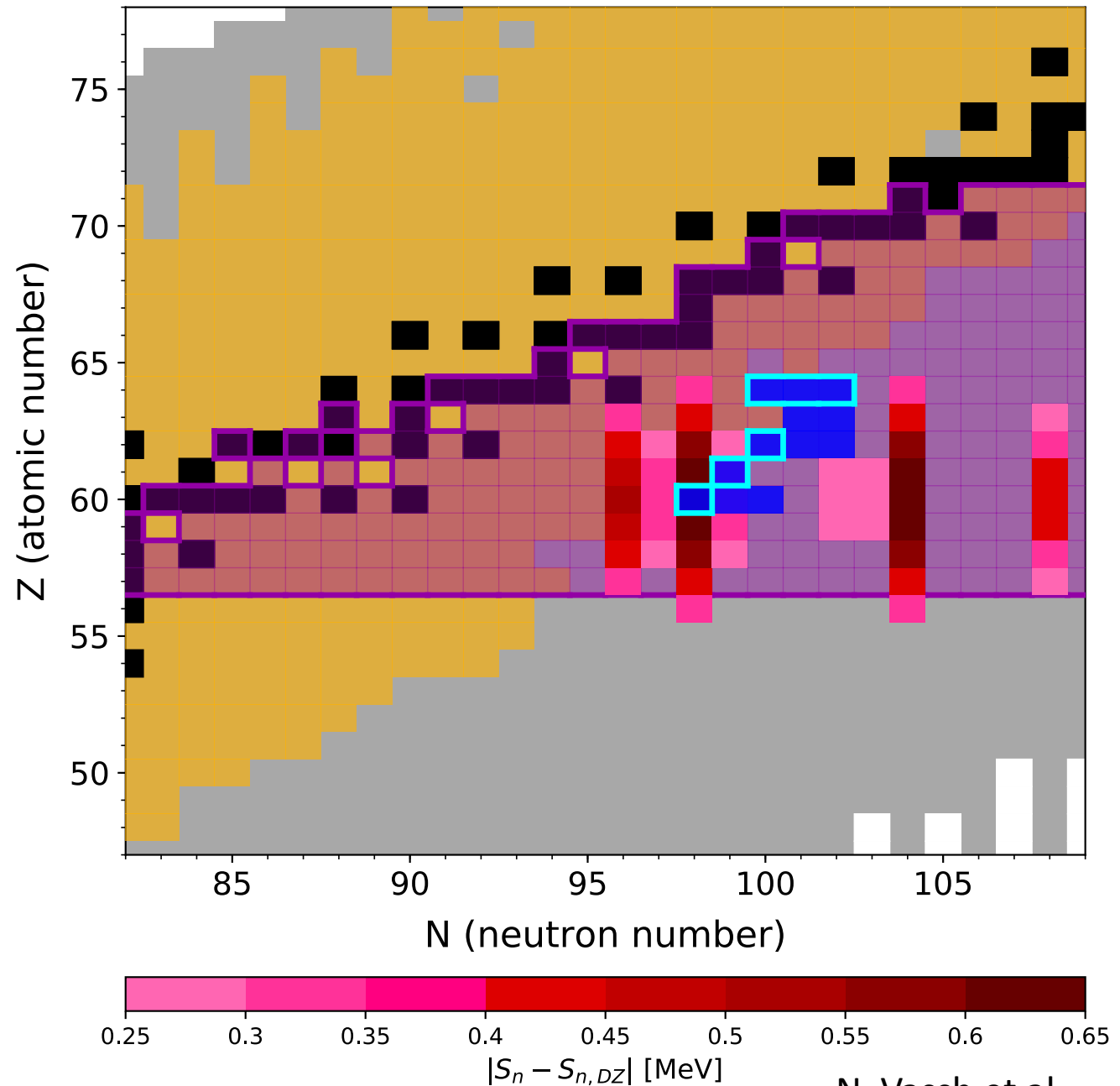
Jyväskylä

CPT at CARIBU

Theory (ND, NCSU, LANL):

Markov Chain Monte Carlo Mass Corrections to the Duflo-Zuker Model which **reproduce the observed rare-earth abundance peak**

(right: result with $s/k=30$, $\tau=70$ ms, $Y_e=0.2$)



N. Vassh et al
(in preparation)

Standard r -process calculation

Astrophysical conditions

Fission Yields

Rates (n capture, β -decay, fission....)

Nuclear masses



Nucleosynthesis code
(PRISM)



**Abundance
prediction**

Reverse Engineering *r*-process calculation

Astrophysical conditions

Fission Yields

Rates (n capture, β -decay, fission....)



Nucleosynthesis code
(PRISM)



Abundance
prediction

Nuclear masses



Markov Chain Monte
Carlo (MCMC)
Likelihood function



MCMC procedure

- Monte Carlo mass corrections

$$M(Z, N) = M_{DZ}(Z, N) + a_N e^{-(Z-c)^2/2f}$$

- Check: $\sigma_{\text{rms}}^2(M_{\text{AME12}}, M) \leq \sigma_{\text{rms}}^2(M_{\text{AME12}}, M_{DZ})$

- Check:

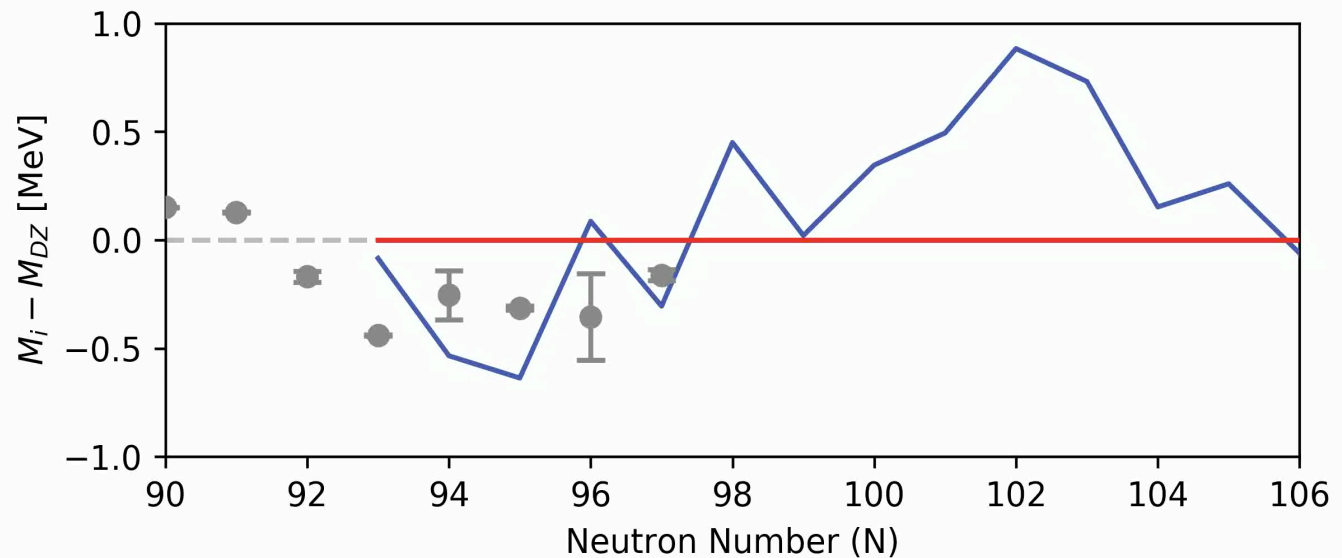
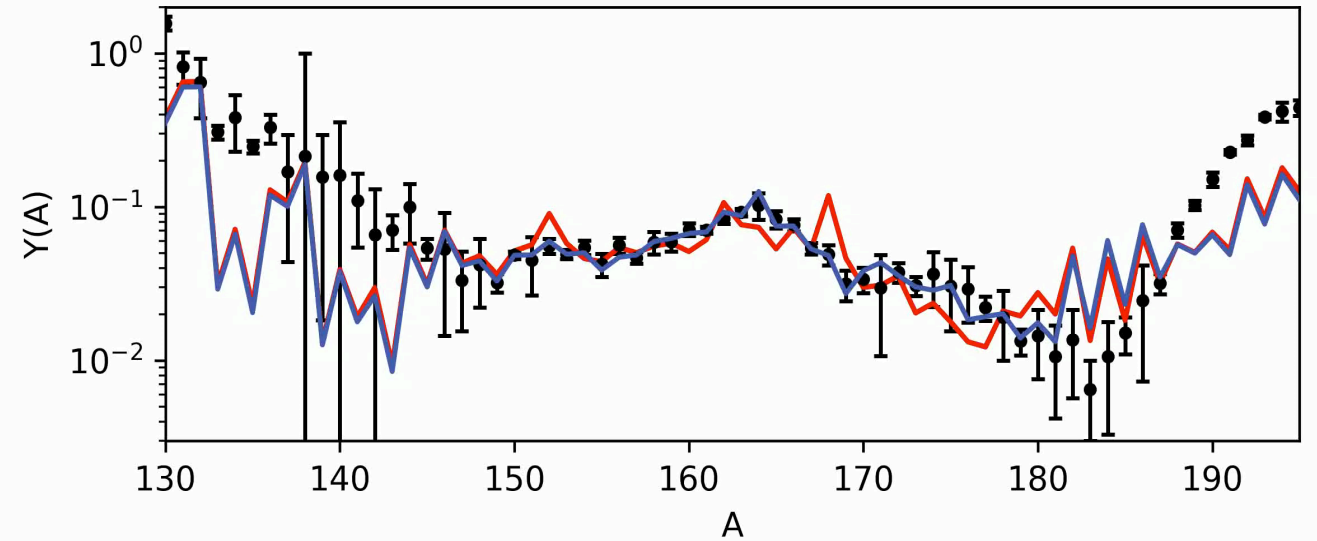
$$D_n(Z, A) = (-1)^{A-Z+1} (S_n(Z, A+1) - S_n(Z, A)) > 0$$

- Update nuclear quantities and rates
- Perform nucleosynthesis calculation

- Calculate $\chi^2 = \sum_{A=150}^{180} \frac{(Y_{\odot,r}(A) - Y(A))^2}{\Delta Y(A)^2}$

- Update parameters OR revert to last success

$$\mathcal{L}(m) = \exp\left(-\frac{\chi^2(m)}{2}\right) \rightarrow \alpha(m) = \frac{\mathcal{L}(m)}{\mathcal{L}(m-1)}$$

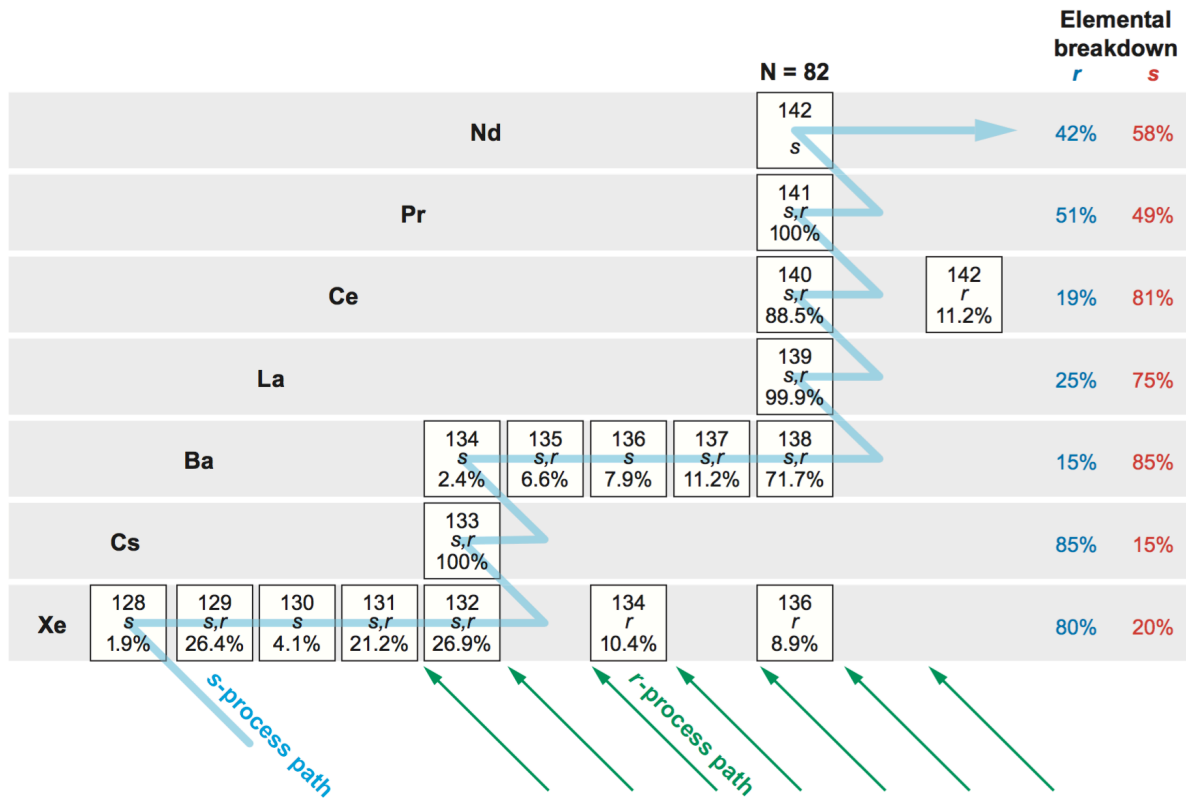


Black – solar abundance data

Grey – AME 2012 data

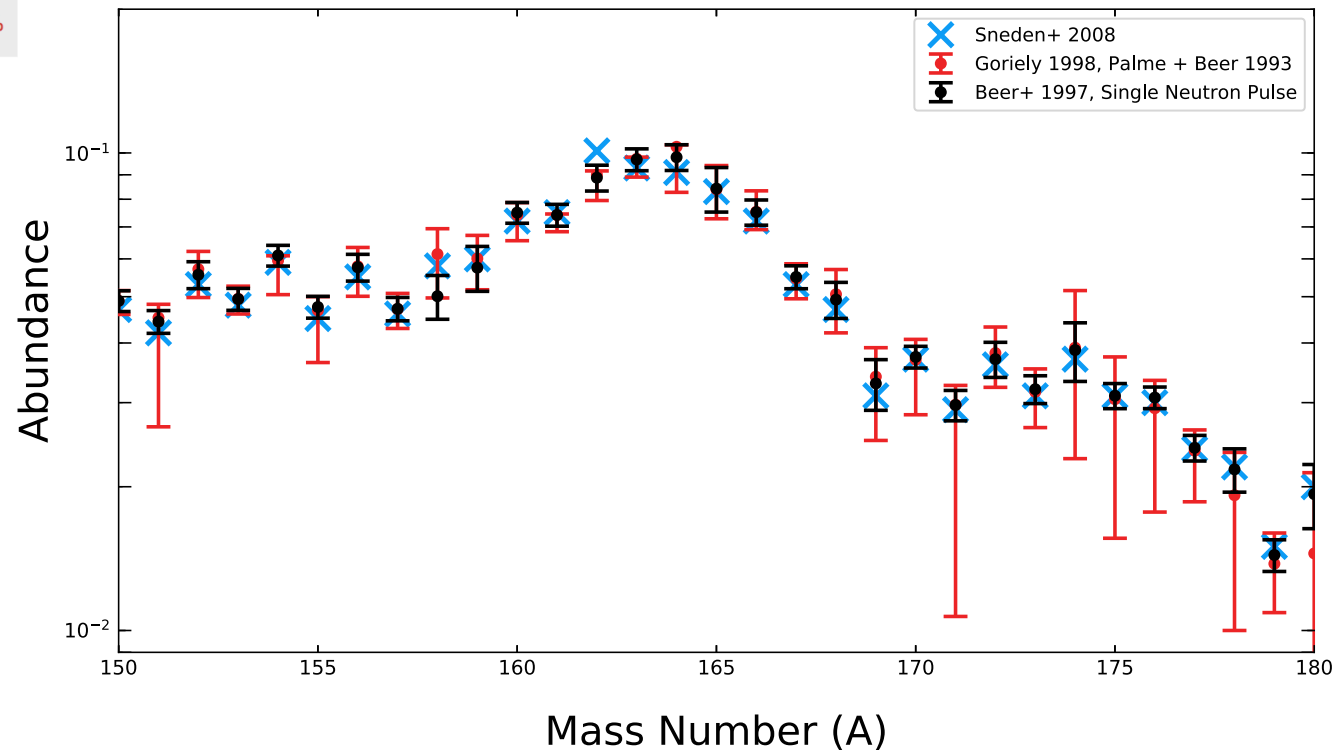
Red – values at current step

Blue – best step of entire run



Sneden, Cowan, and Gallino (2008)

Sensitivity to Solar Data: uncertainty from the s-process subtraction

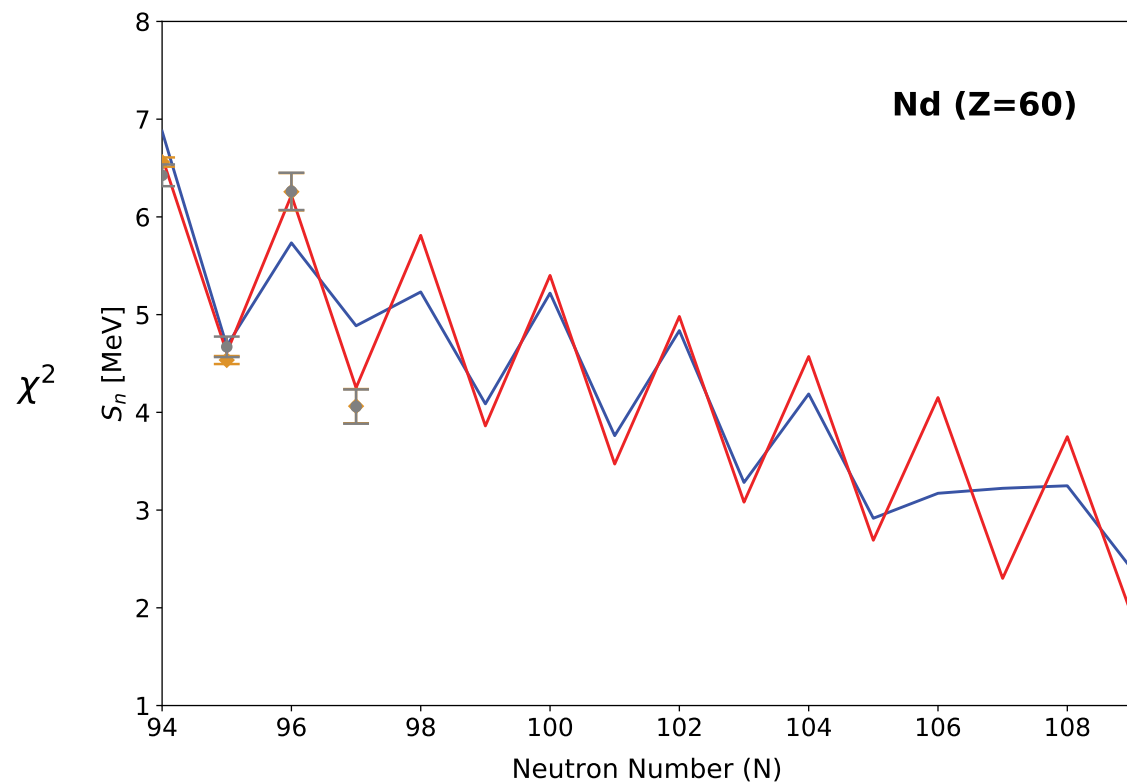
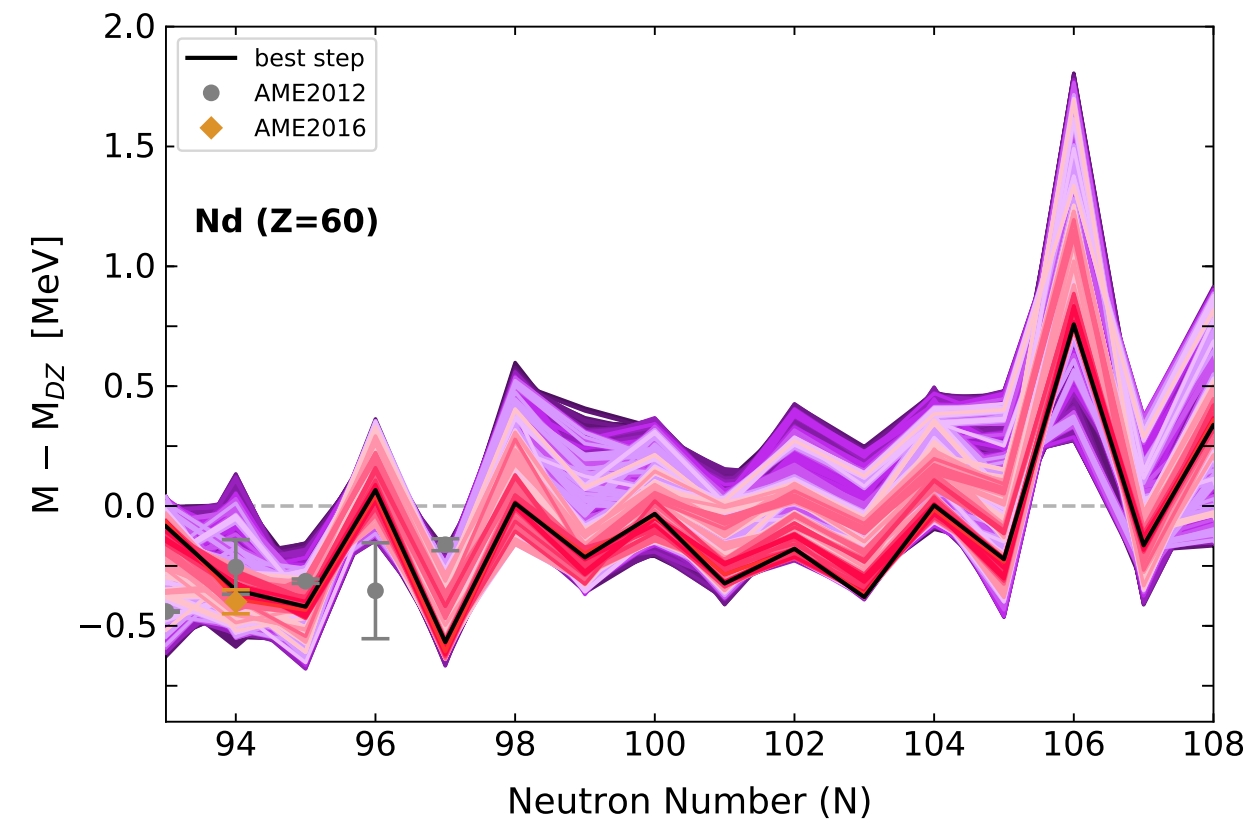


Parallel Chains Method of MCMC

- Highly correlated parameters → long convergence time for a single run
- Multiple independent runs allow for a thorough search of parameter space
- Well-defined statistics when combine results from independent runs



Example of a discarded, unphysical MCMC solution



Vassh et al (in preparation)

Dynamic Mechanism Of Rare-Earth Peak Formation

Detailed balance implies

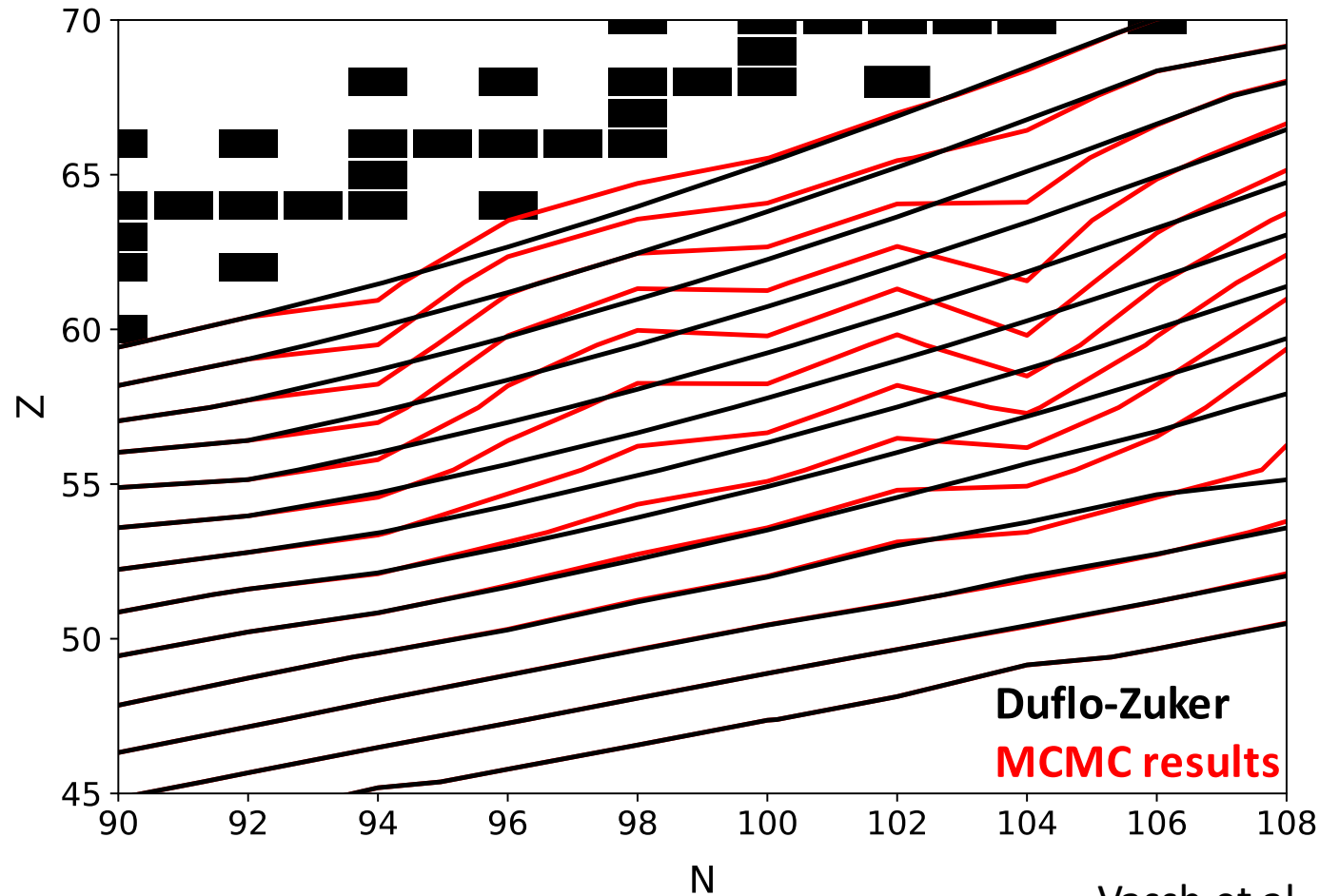
$$(\gamma, n) \propto e^{-S_n/kT}$$



r-process path tends to lie along contours of constant separation energy



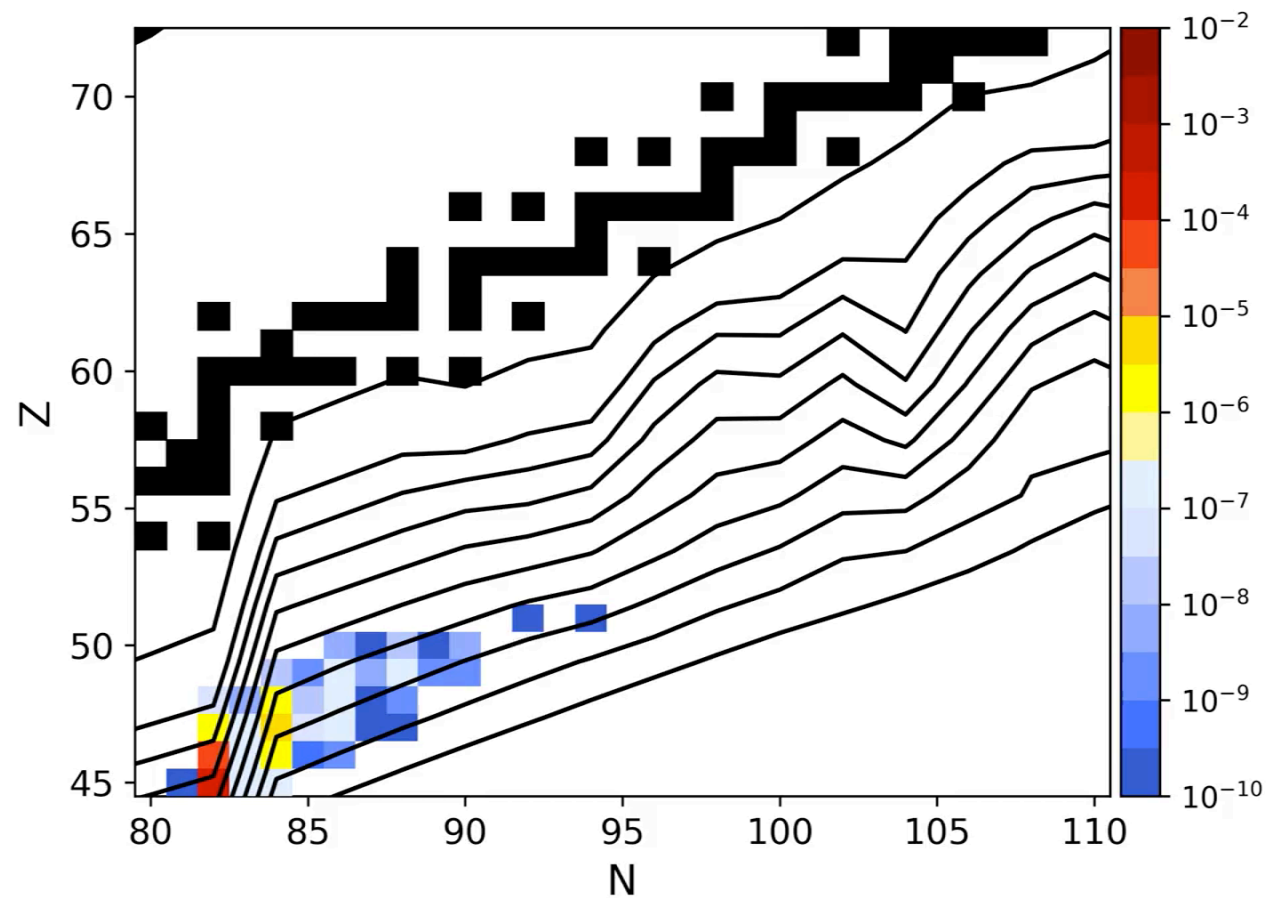
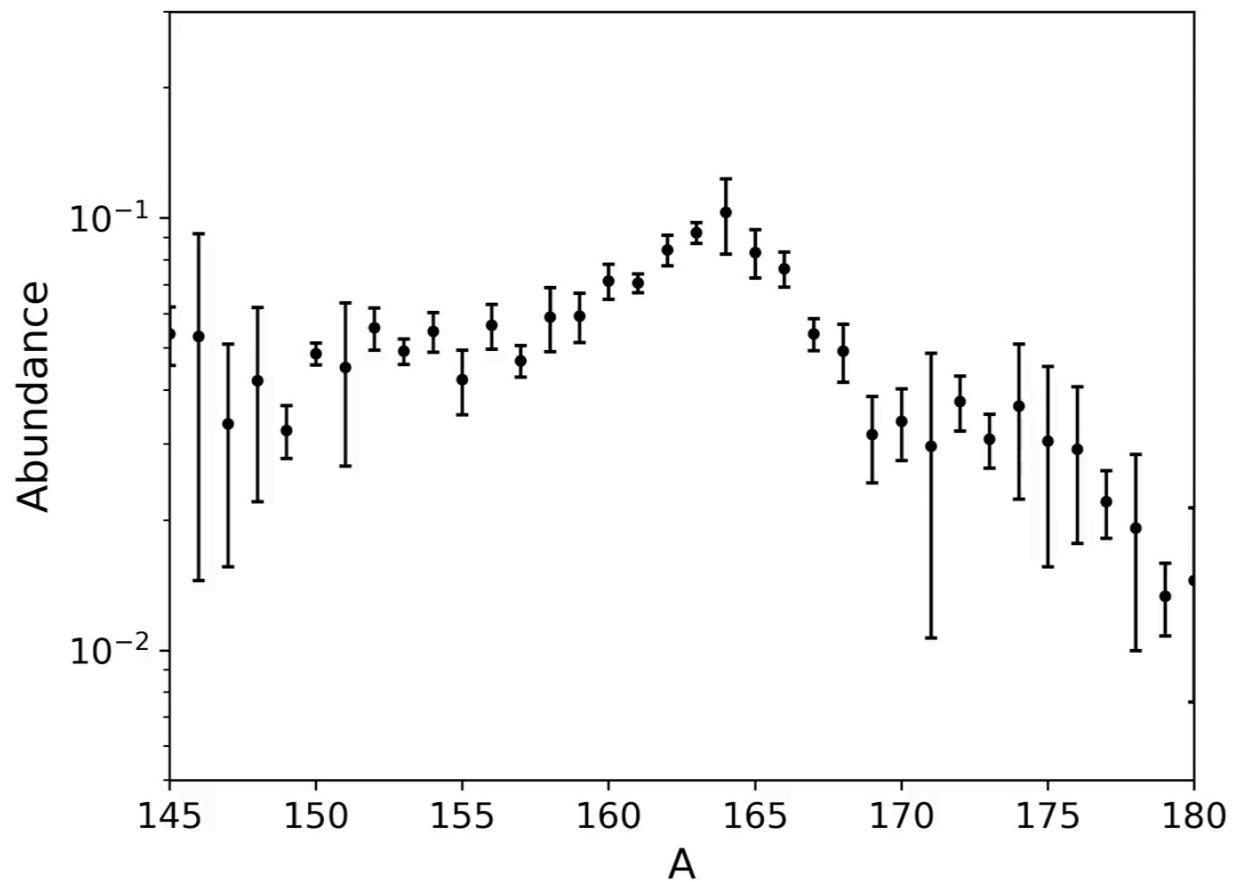
Pile-up of material at kinks



Vassh et al
(in preparation)

NOTE: FISSION is the other possible means of REP formation

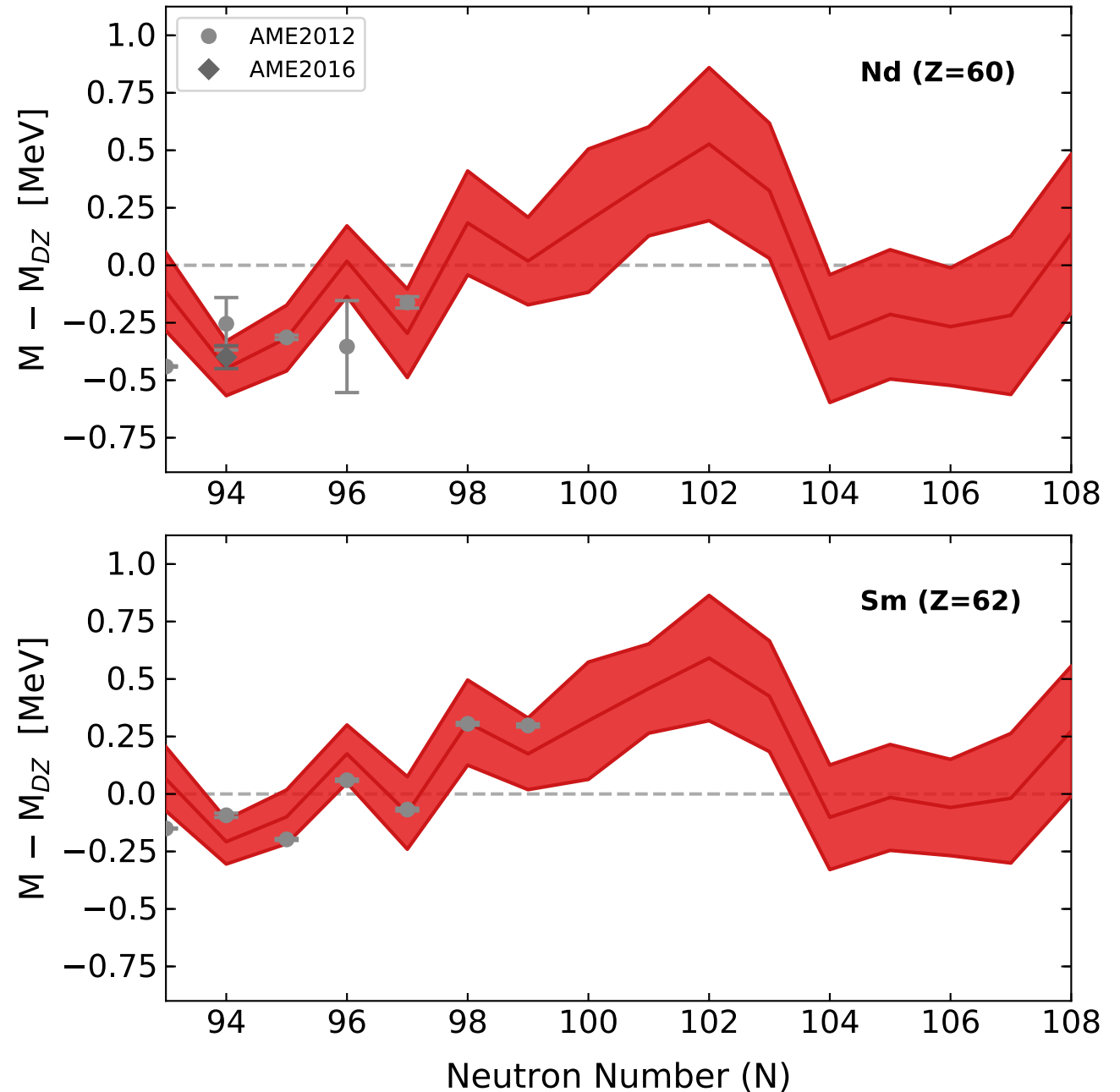
Peak Formation with an MCMC Mass Solution



Results

- Astrophysical trajectory:
hot, low entropy **wind** as from a NSM
accretion disk
($s/k=30$, $\tau=70$ ms, $Y_e=0.2$)
- 50 parallel, independent MCMC runs;
Average run $\chi^2 \sim 23$

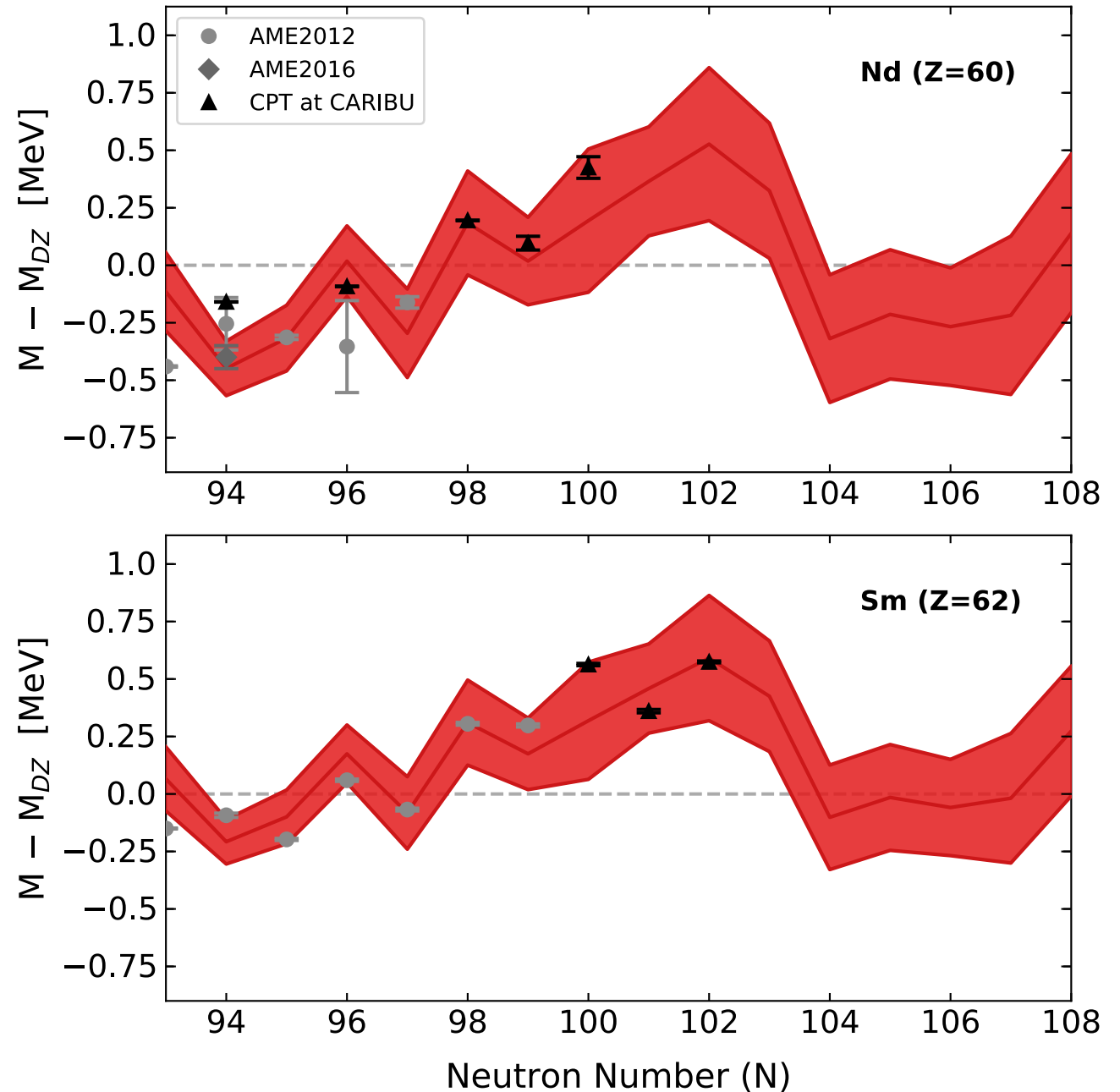
Orford, Vassh, Clark, McLaughlin, Mumpower,
Savard, Surman, Aprahamian, Buchinger,
Burkey, Gorelov, Hirsh, Klimes, Morgan,
Nystrom, and Sharma
(submitted to PRL)



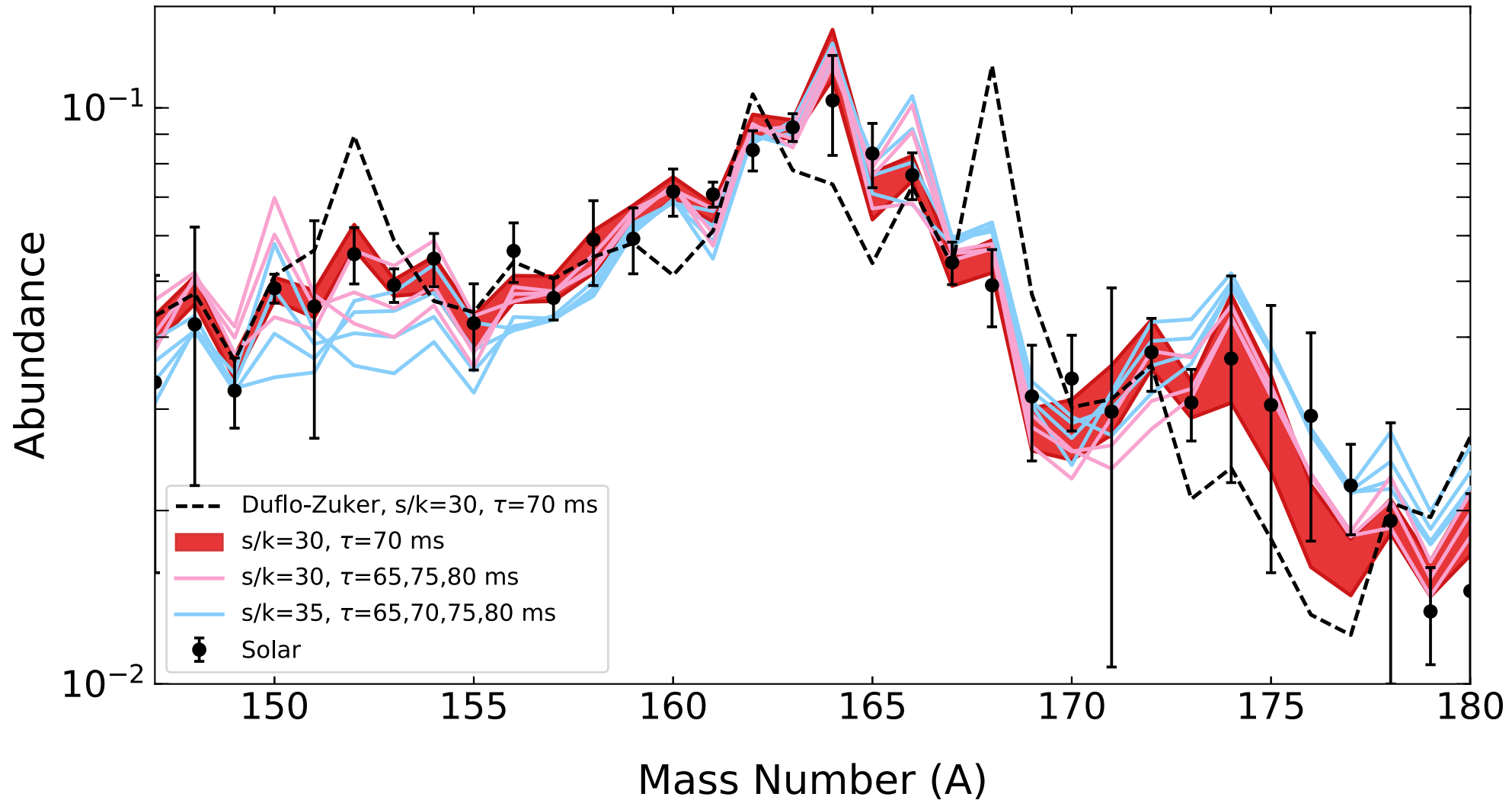
Results

- Astrophysical trajectory:
hot, low entropy **wind** as from a NSM
accretion disk
($s/k=30$, $\tau=70$ ms, $Y_e=0.2$)
- 50 parallel, independent MCMC runs;
Average run $\chi^2 \sim 23$

Orford, Vassh, Clark, McLaughlin, Mumpower,
Savard, Surman, Aprahamian, Buchinger,
Burkey, Gorelov, Hirsh, Klimes, Morgan,
Nystrom, and Sharma
(submitted to PRL)



Rare-Earth Peak with MCMC solutions

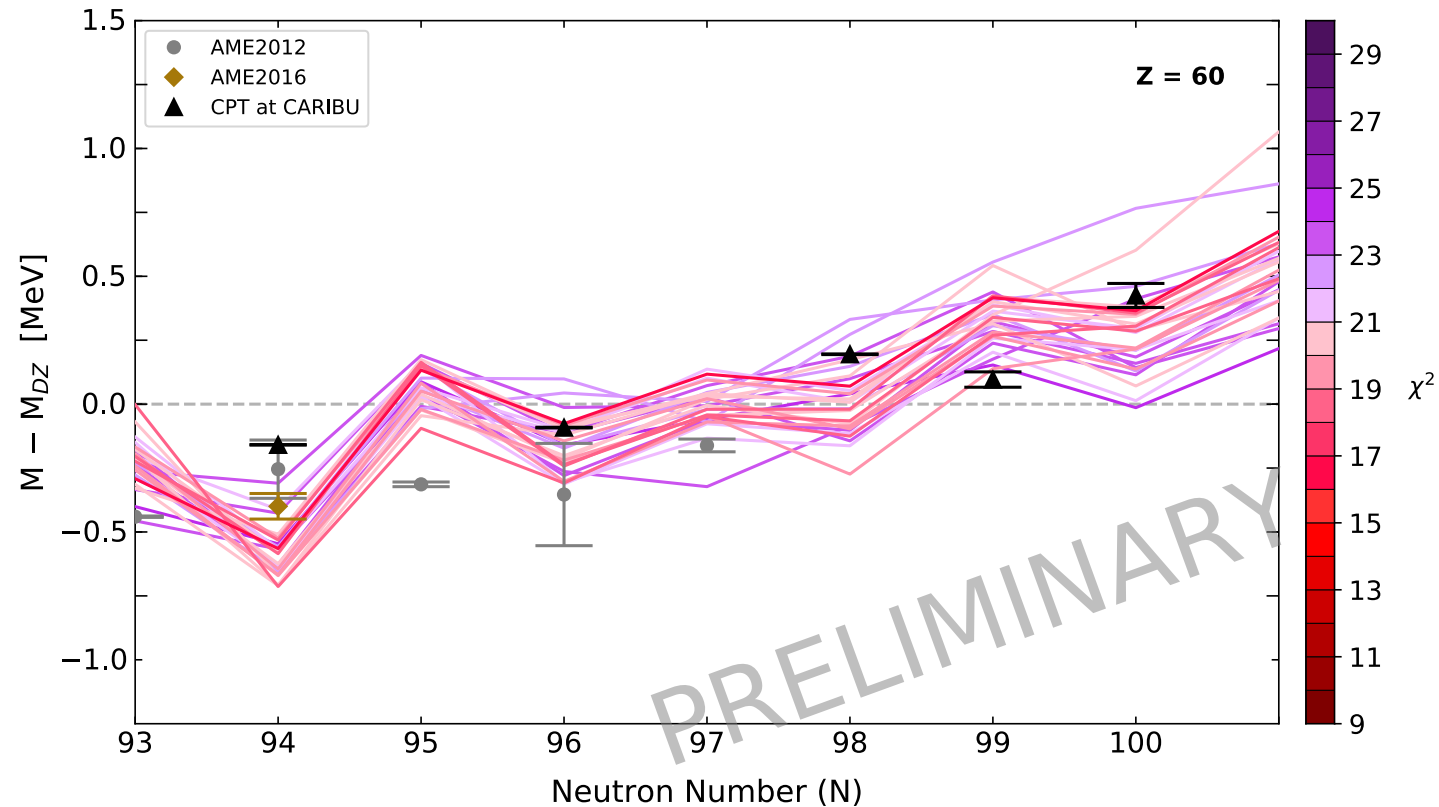


Preliminary Results

- Astrophysical trajectory: n-rich NSM **dynamical** ejecta with nuclear reheating
- 50 independent MCMC runs complete



30 Runs (Best Step Colored by χ^2)



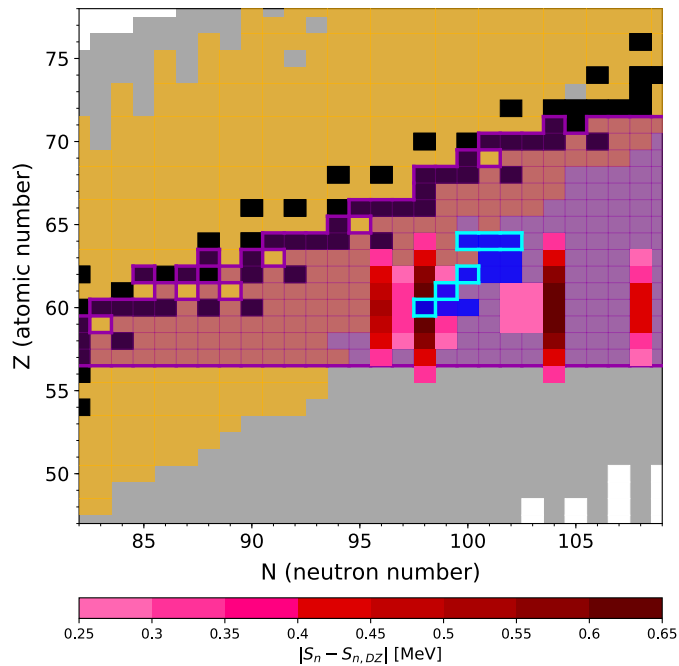
Vassh et al
(in preparation)

Nucleosynthesis in Neutron Star Mergers: Many Open Questions

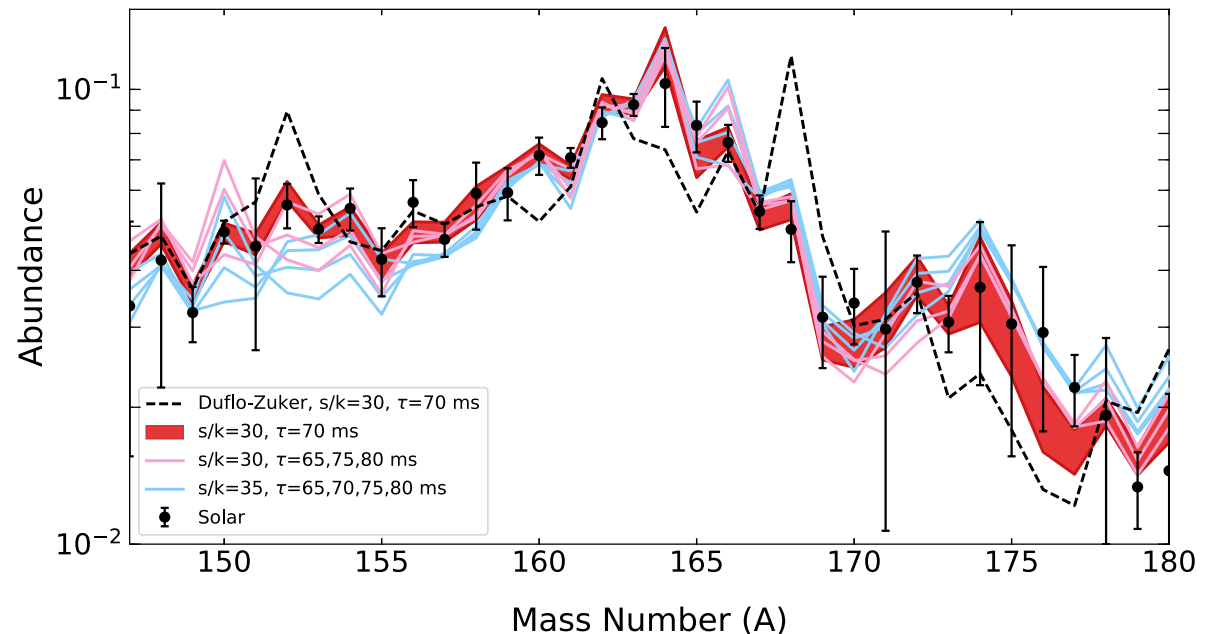
- Can mergers account for all the *r*-process material observed in the galaxy?
- Are precious metals such as gold produced in sufficient amounts?
- Are actinides produced?
- Where within the merger environment does nucleosynthesis occur and under what specific conditions?
- How does the rare-earth peak form?

Nucleosynthesis in Neutron Star Mergers: Many Open Questions

- Can mergers account for all the r -process material observed in the galaxy?
- Are precious metals such as gold produced in sufficient amounts?
- Are actinides produced?
- Where within the merger environment does nucleosynthesis occur and under what specific conditions?
- How does the rare-earth peak form?



Vassh et al (in preparation)



Orford, Vassh, et al (submitted to PRL)

Back-up Slides



Fission In R-process Elements

The FIRE collaboration explores the role of fission in the rapid neutron capture or r-process of nucleosynthesis

BROOKHAVEN
NATIONAL LABORATORY

McCutchan and Sonzogni



Lawrence
Livermore
National
Laboratory

Vogt and Schunck



UNIVERSITY OF
NOTRE DAME

Vassh and Surman



**Mumpower, Jaffke,
Verriere, Kawano, Talou,
and Hayes-Sterbenz**

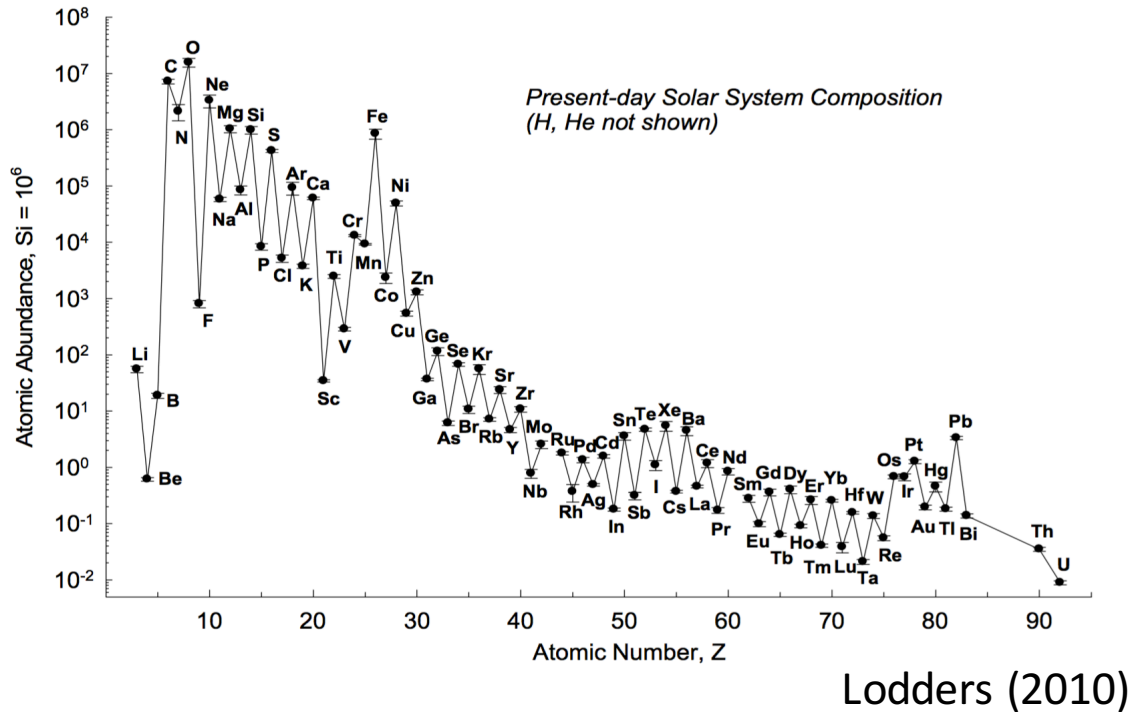


McLaughlin and Zhu

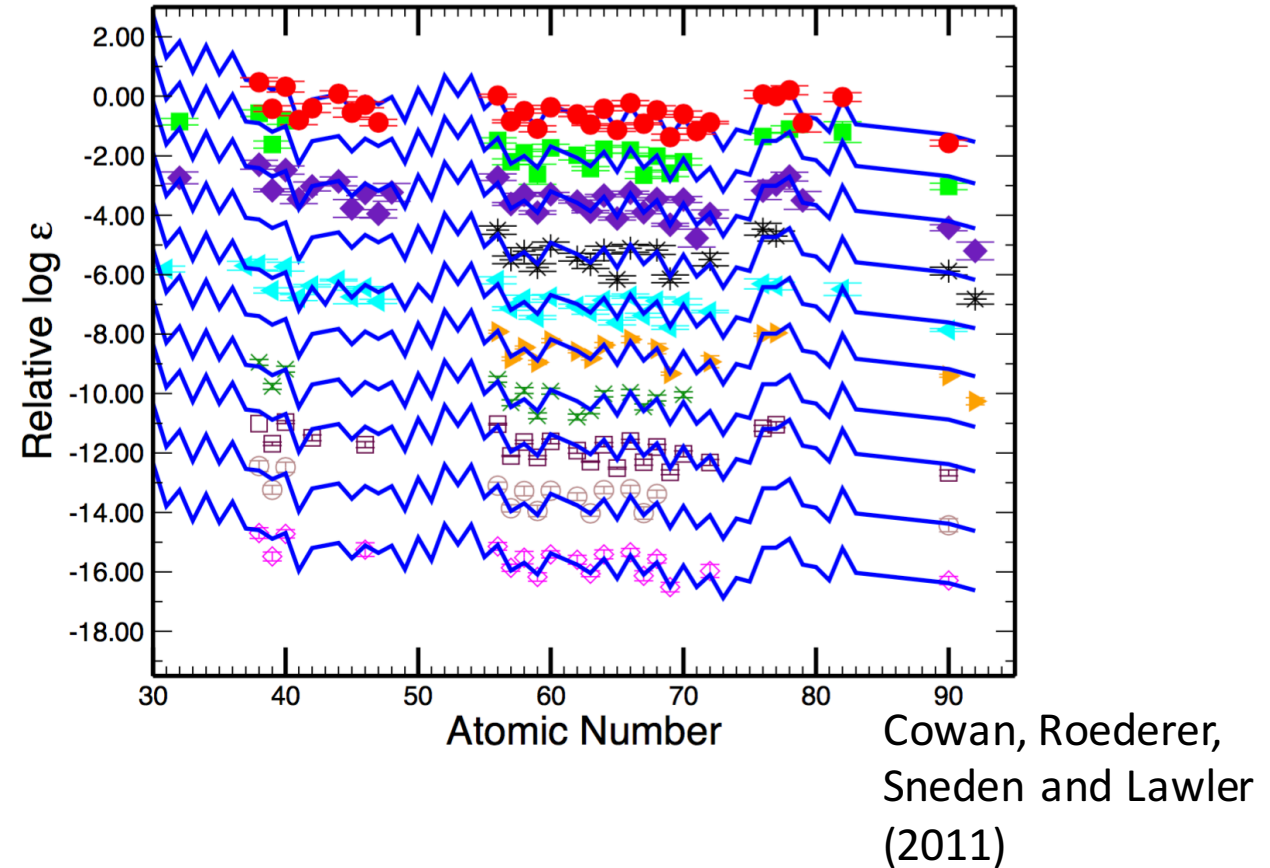


Observed Elemental Abundances

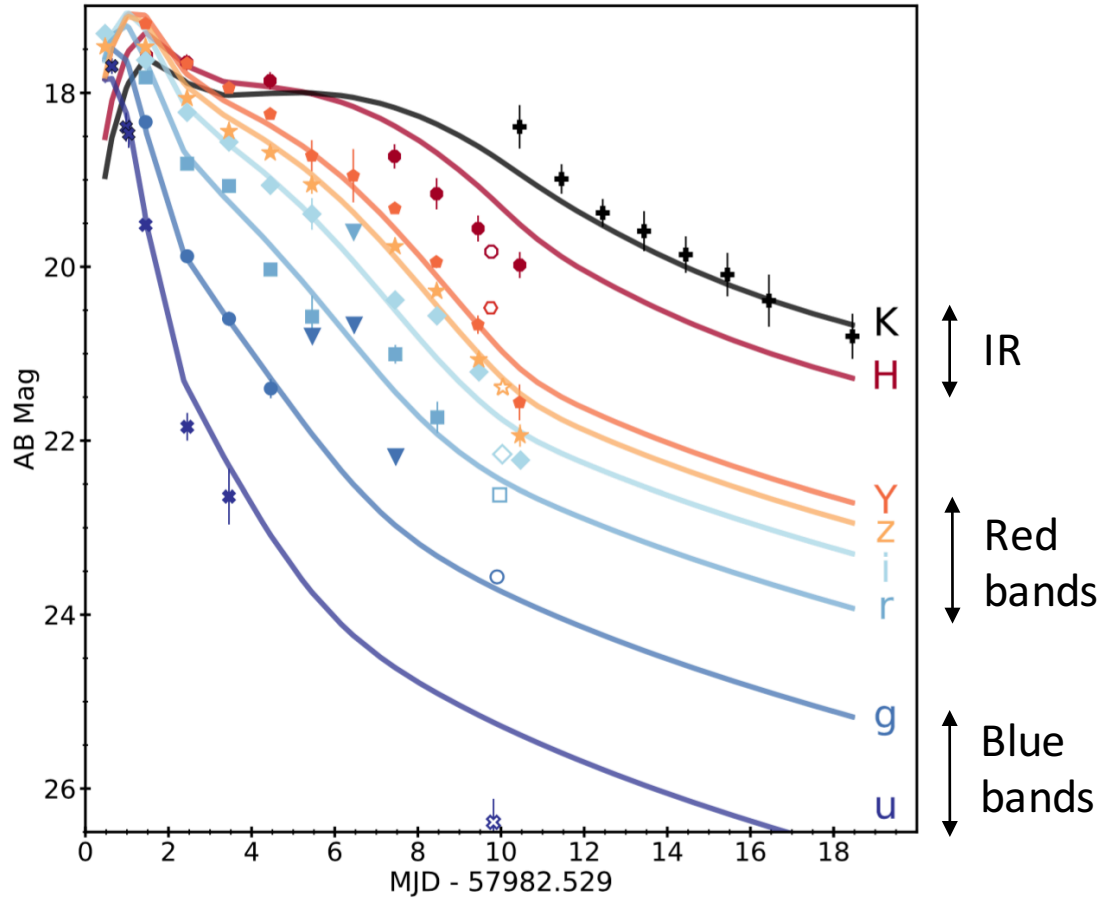
Solar System



10 *r*-process rich halo stars

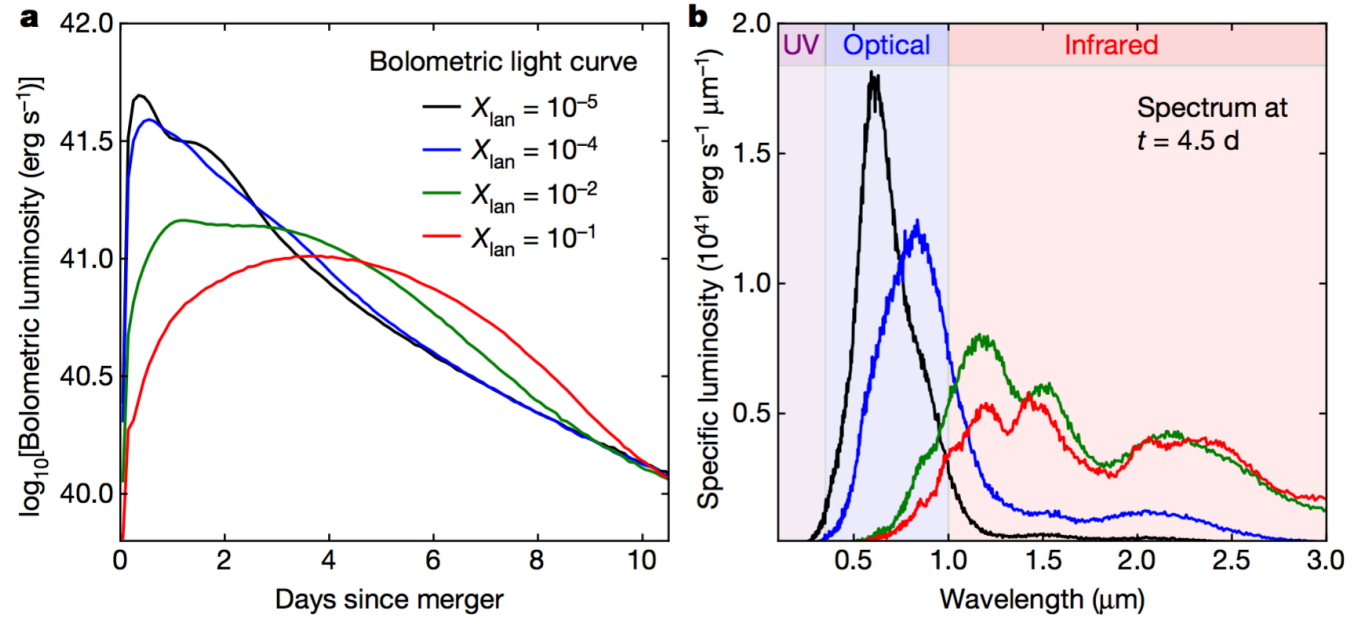


Lanthanide production in GW170817: “red” kilonova



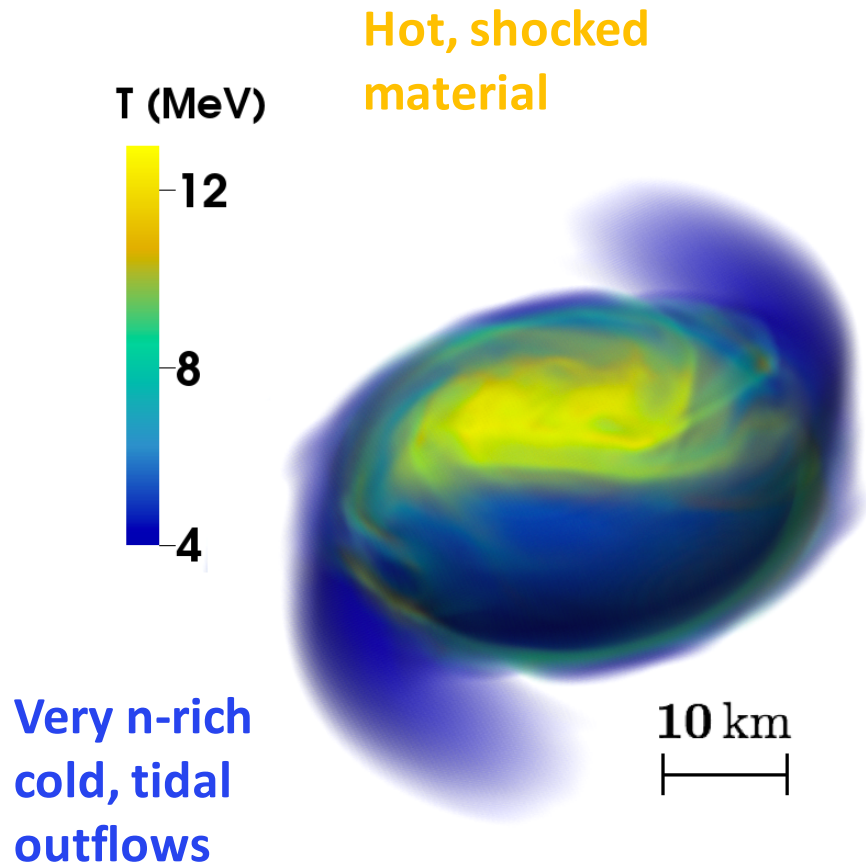
Cowperthwaite et al (ApJL 2017)

Lanthanide mass fraction \uparrow , opacity \uparrow , longer duration light curve shifted toward infrared



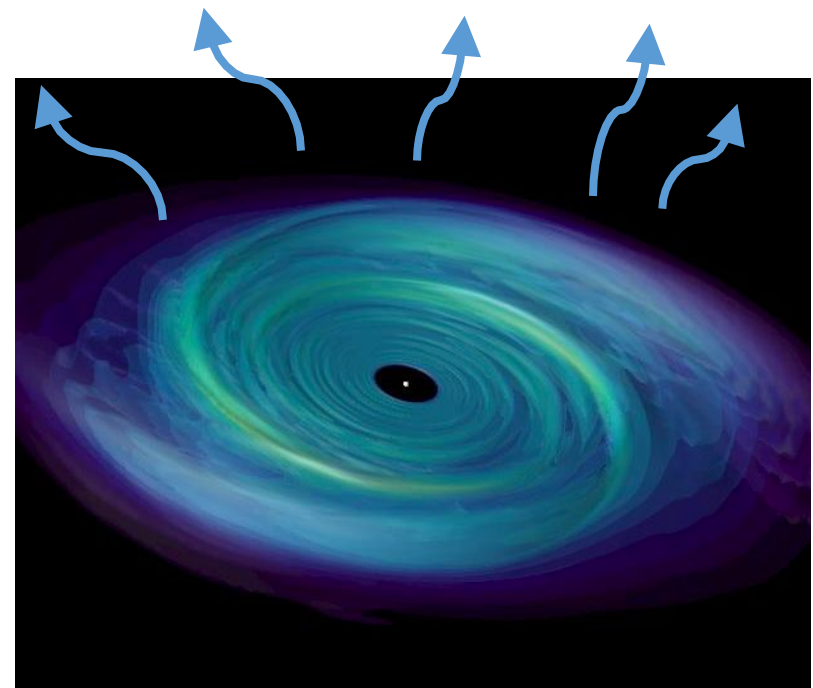
Kasen et al (*Nature* 2017)

r-process sites within a Neutron Star Merger



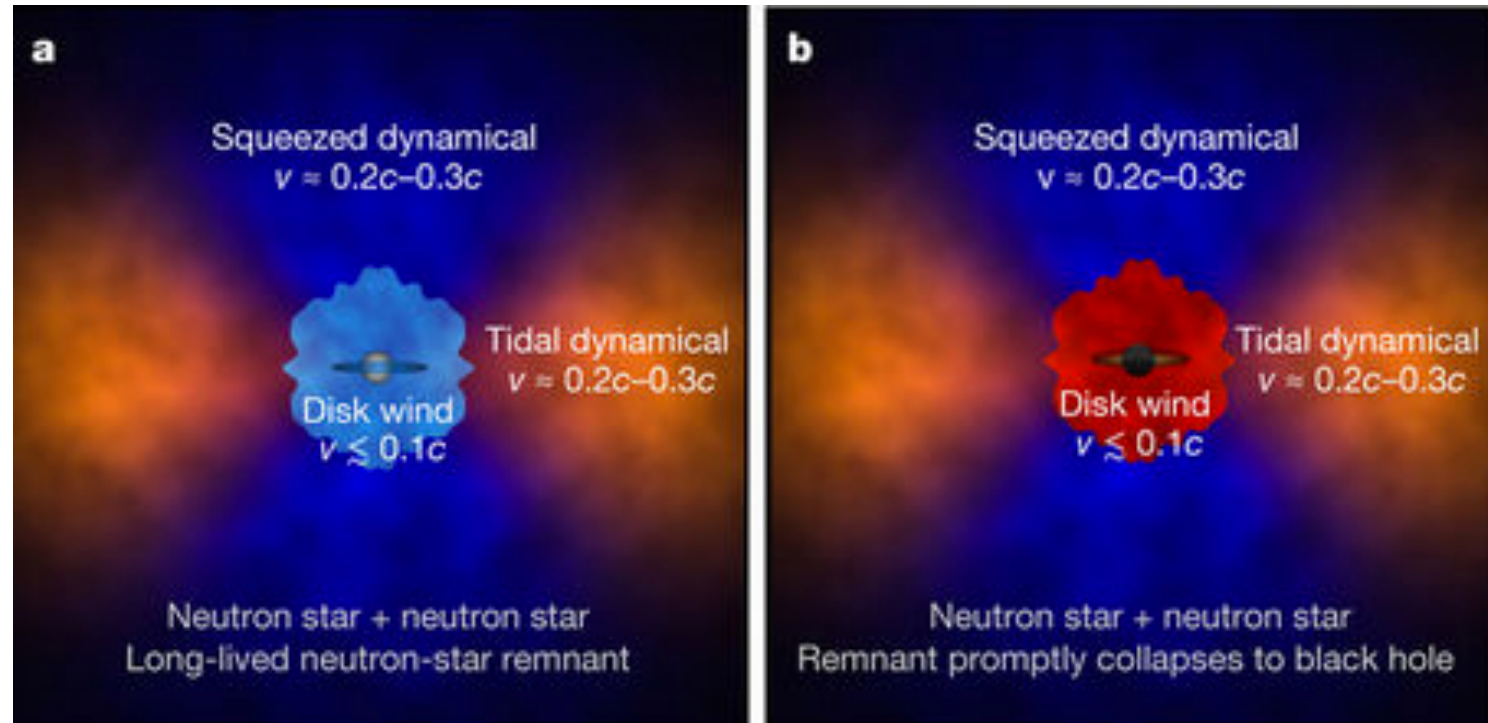
Foucart et al (2016)

**Accretion disk winds –
exact driving mechanism
and neutron richness varies**



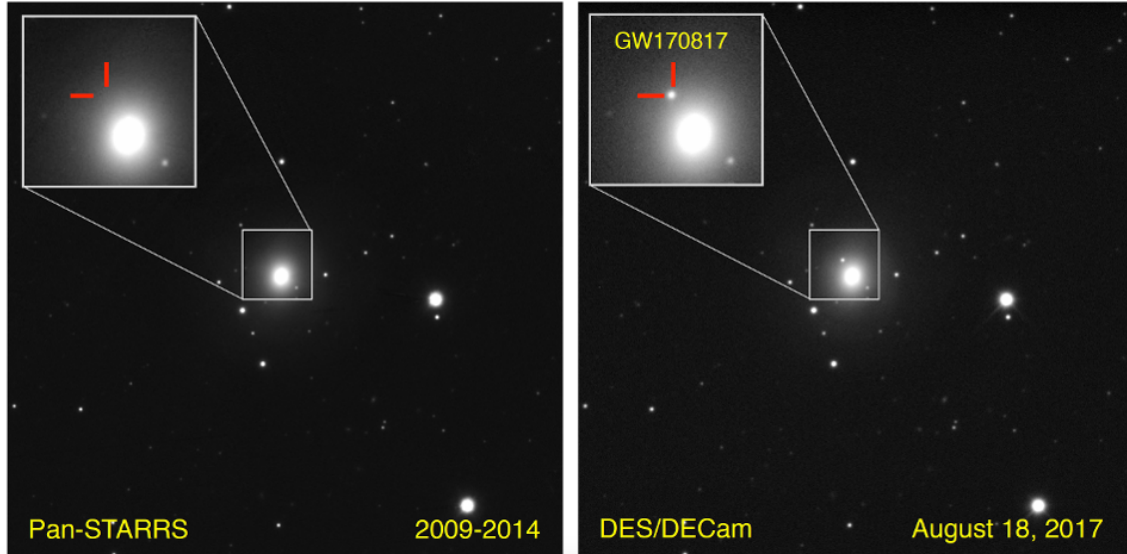
Owen and Blondin

r -process sites within a Neutron Star Merger



Kasen, Metzger, Barnes,
Quataert, and Ramirez-Ruiz
(*Nature* 2017)

GW170817 and r -process uncertainties from nuclear physics



Reference	$m_{\text{dyn}} [M_{\odot}]$	$m_w [M_{\odot}]$
Abbott et al. (2017a)	0.001 – 0.01	–
Arcavi et al. (2017)	–	0.02 – 0.025
Cowperthwaite et al. (2017)	0.04	0.01
Chornock et al. (2017)	0.035	0.02
Evans et al. (2017)	0.002 – 0.03	0.03 – 0.1
Kasen et al. (2017)	0.04	0.025
Kasliwal et al. (2017b)	> 0.02	> 0.03
Nicholl et al. (2017)	0.03	–
Perego et al. (2017)	0.005 – 0.01	10^{-5} – 0.024
Rosswog et al. (2017)	0.01	0.03
Smartt et al. (2017)	0.03 – 0.05	0.018
Tanaka et al. (2017a)	0.01	0.03
Tanvir et al. (2017)	0.002 – 0.01	0.015
Troja et al. (2017)	0.001 – 0.01	0.015 – 0.03

Mass fraction range for stable Eu isotopes with 10 mass models

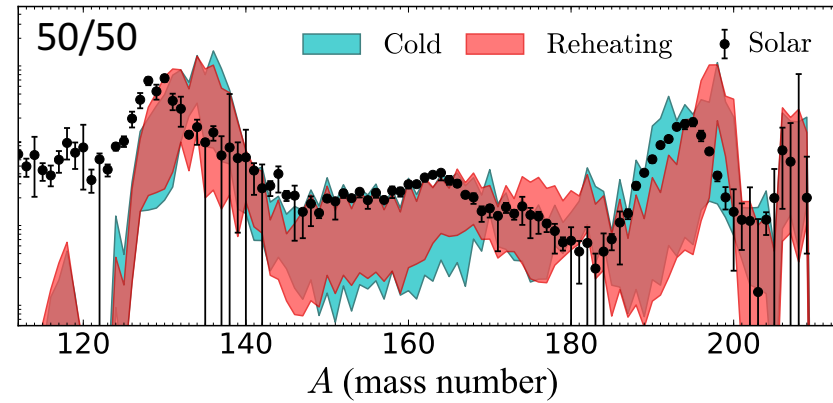
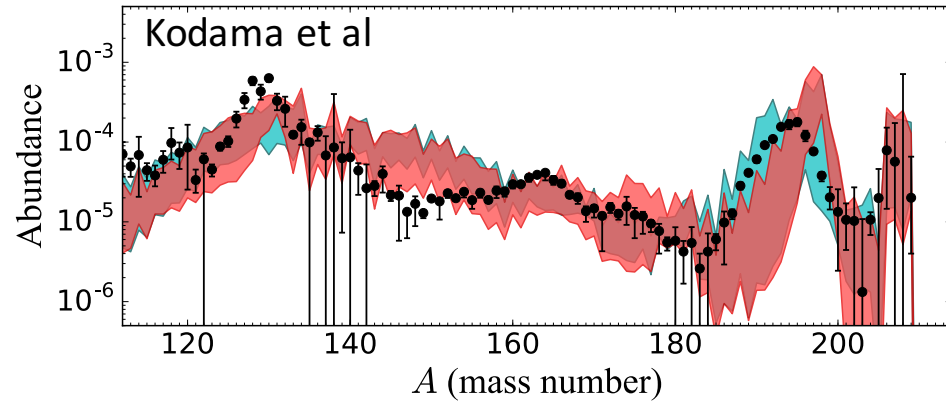
Astrophysical Trajectory	Fission Fragment Distribution	^{151}Eu Mass Fraction [10^{-3}]	^{153}Eu Mass Fraction [10^{-3}]	Relative Abundance Range
Cold outflow (no reheating) (Just et al. 2015)	Kodama & Takahashi (1975)	(5.01 – 11.7)	(3.92 – 8.75)	0.776
	Symmetric Split	(0.083 – 2.65)	(0.12 – 2.84)	3.239
“Slow” ejecta with reheating (Mendoza-Temis et al. 2015)	Kodama & Takahashi (1975)	(2.67 – 13.3)	(1.89 – 9.62)	1.568
	Symmetric Split	(0.19 – 2.09)	(0.24 – 2.23)	2.755

Côté et al (2017) (0.002-0.01) (0.01-0.03)

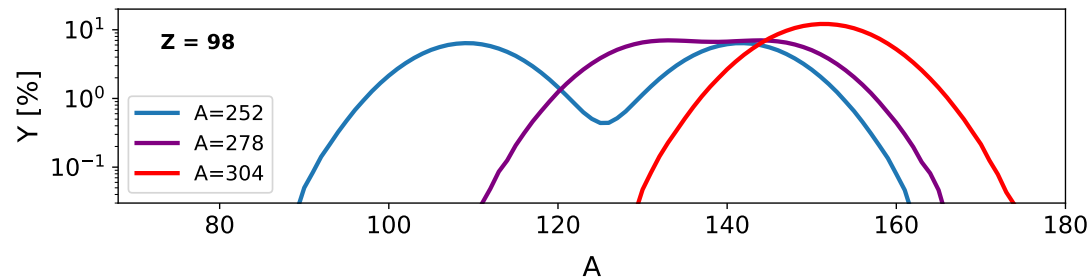
Estimates of ejected mass for GW170817

Côté et al (2017)

Dependence on the Fission Fragment Distribution



Côté et al
(2017)

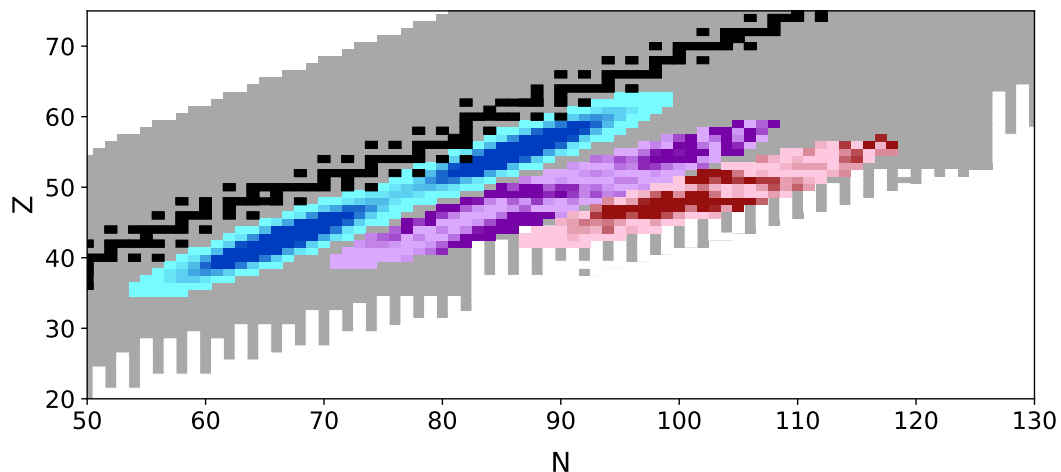


Kodama & Takahashi (1975)

$$Y_{A_f, Z_f}(Z, A)$$

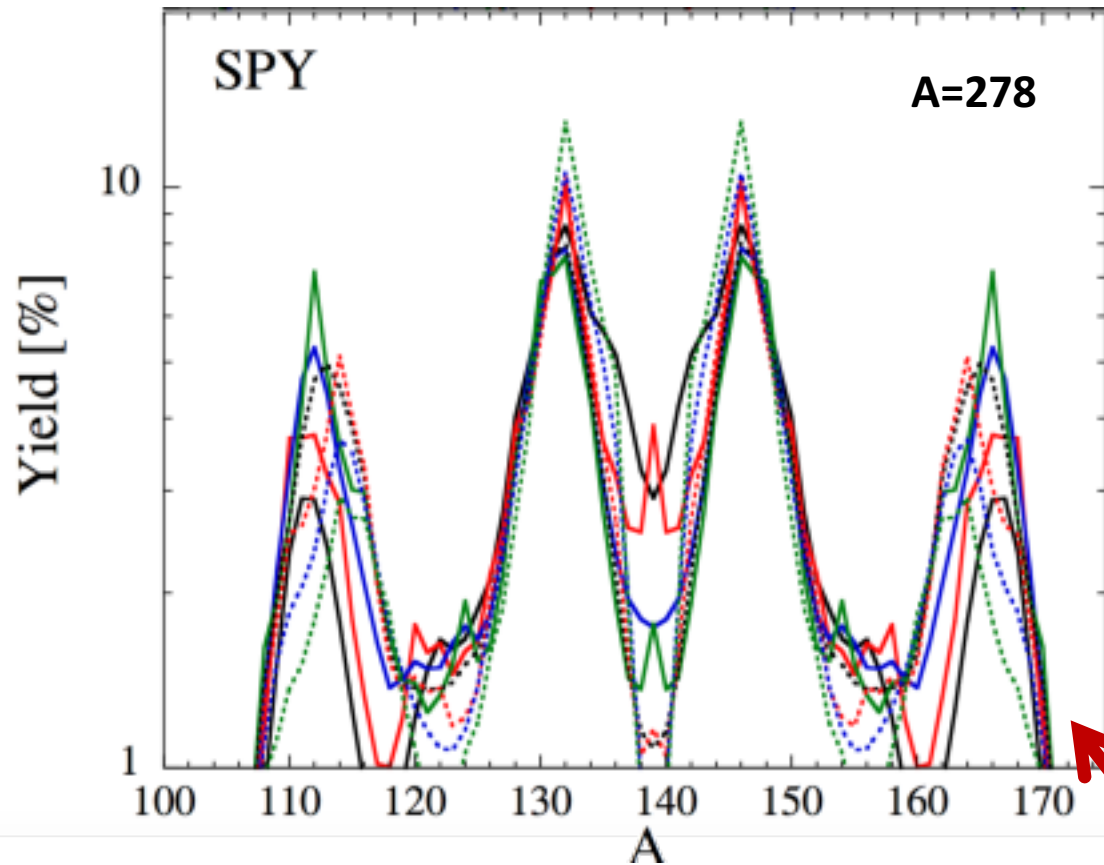
$$\propto \exp\{-(Z - Z_A)^2 / c_Z\}$$

$$\times [\exp\{-(A - A_L)^2 / c_A\} + \exp\{-(A - A_H)^2 / c_A\}]$$

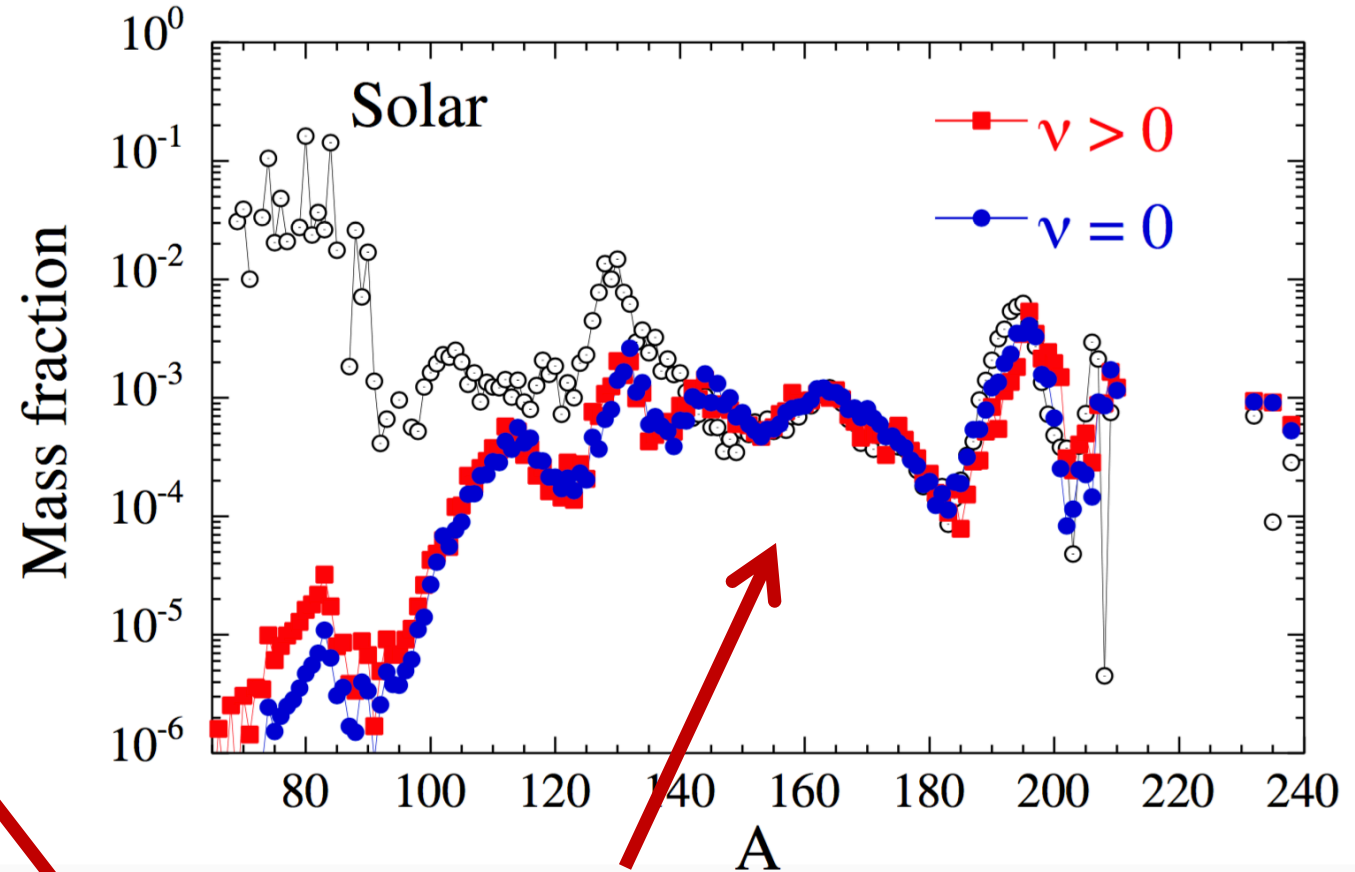


Vassh et al
(in preparation)

Dependence on the Fission Fragment Distribution



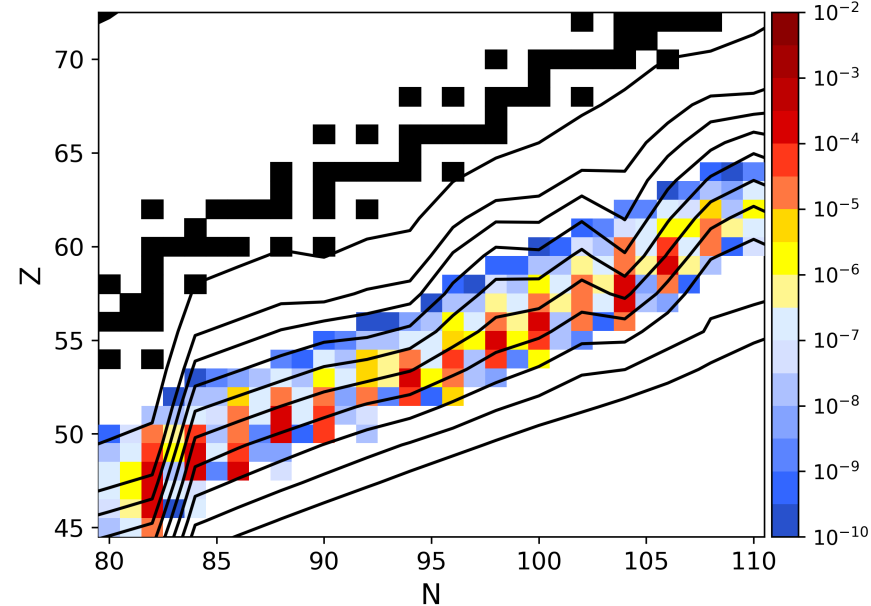
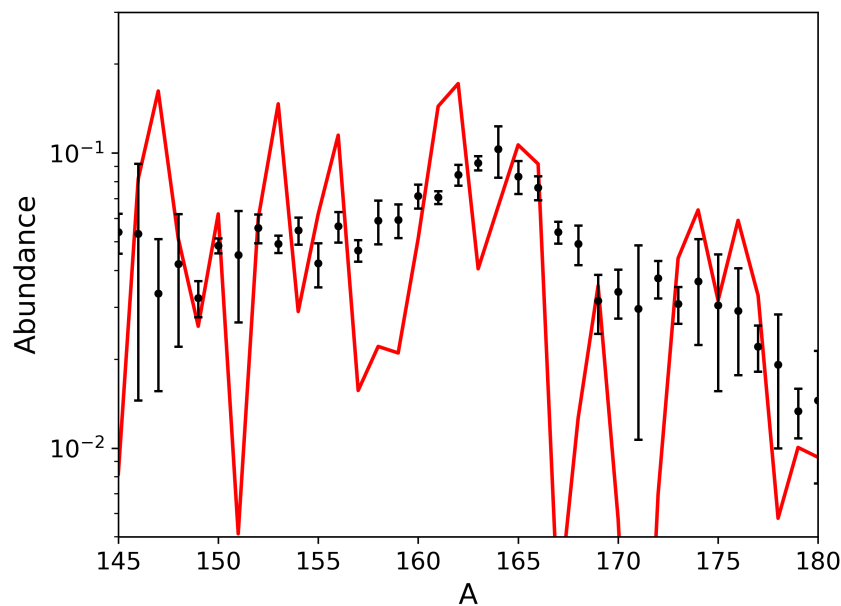
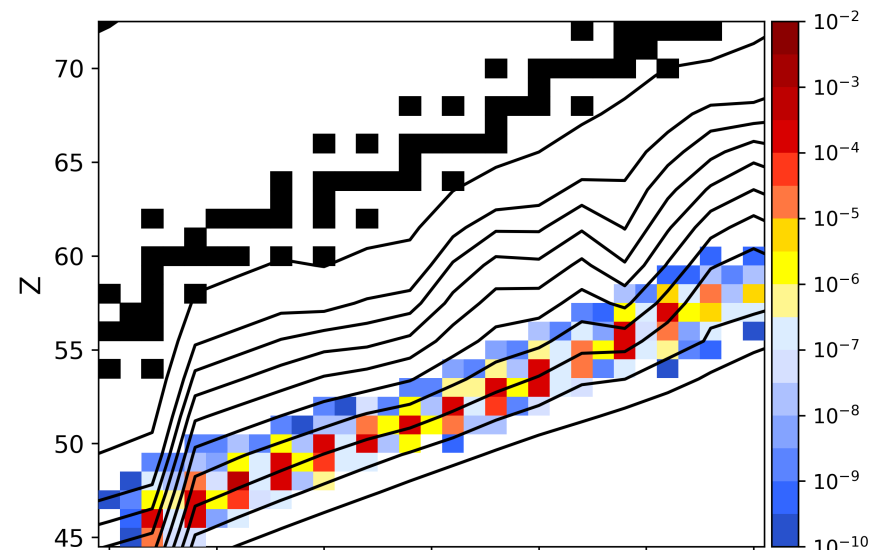
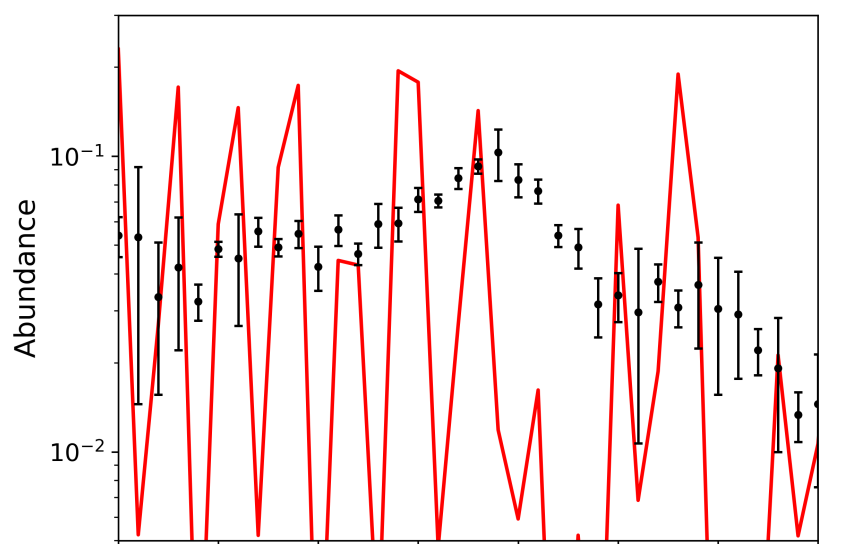
Z=95, Z=96, Z=97, Z=98, Z=99, Z=100,
Z=101, Z=102 (dotted lines – larger Z)



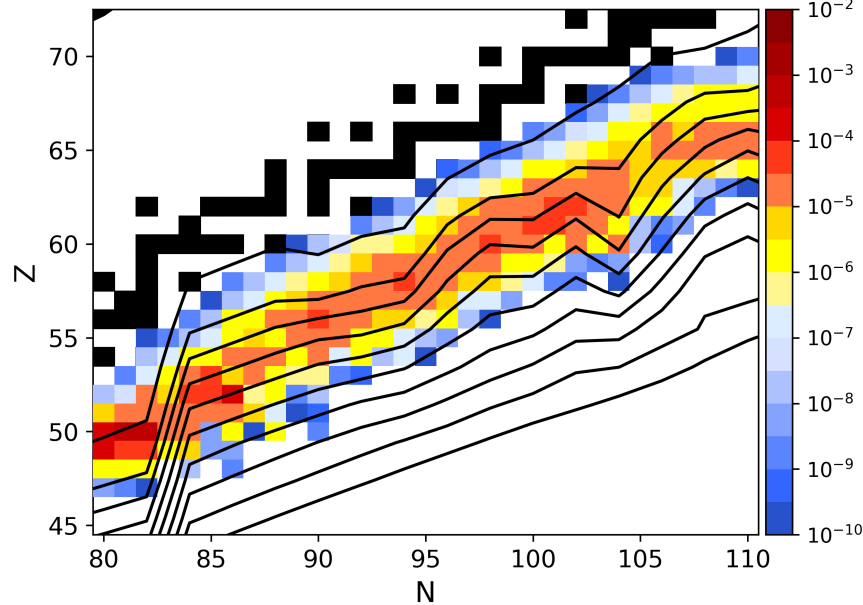
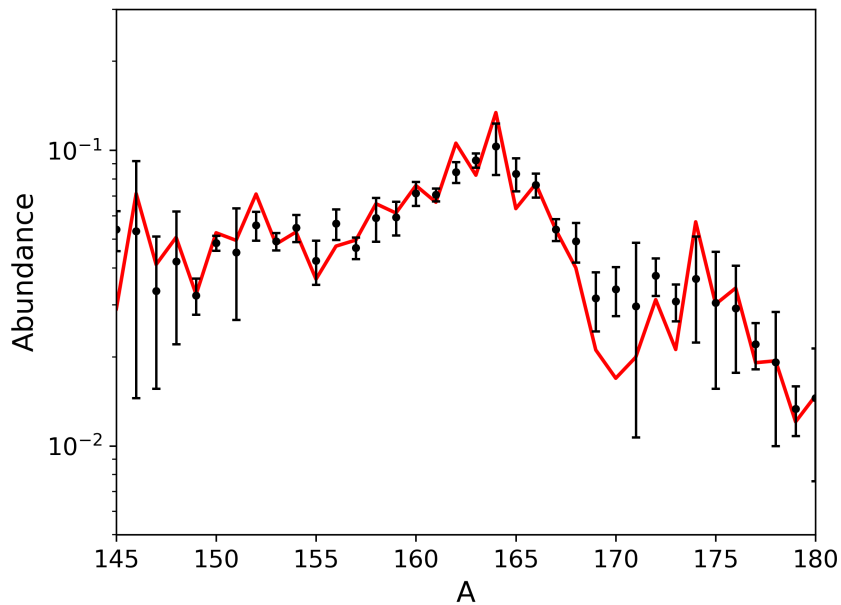
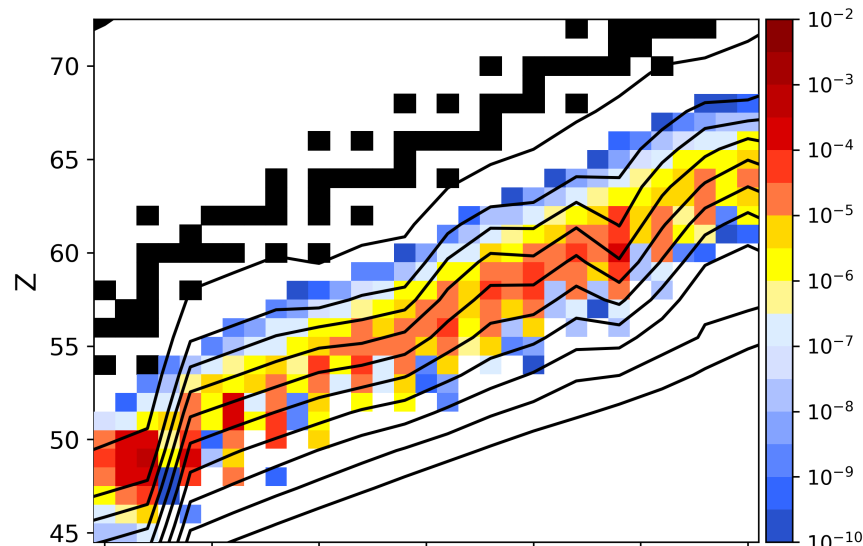
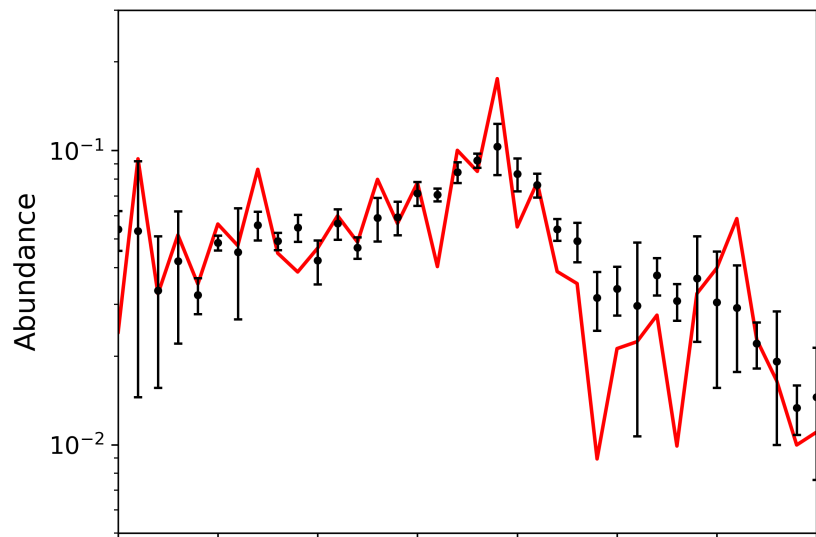
Rare-earth peak can be populated by fission
daughter products of n-rich nuclei

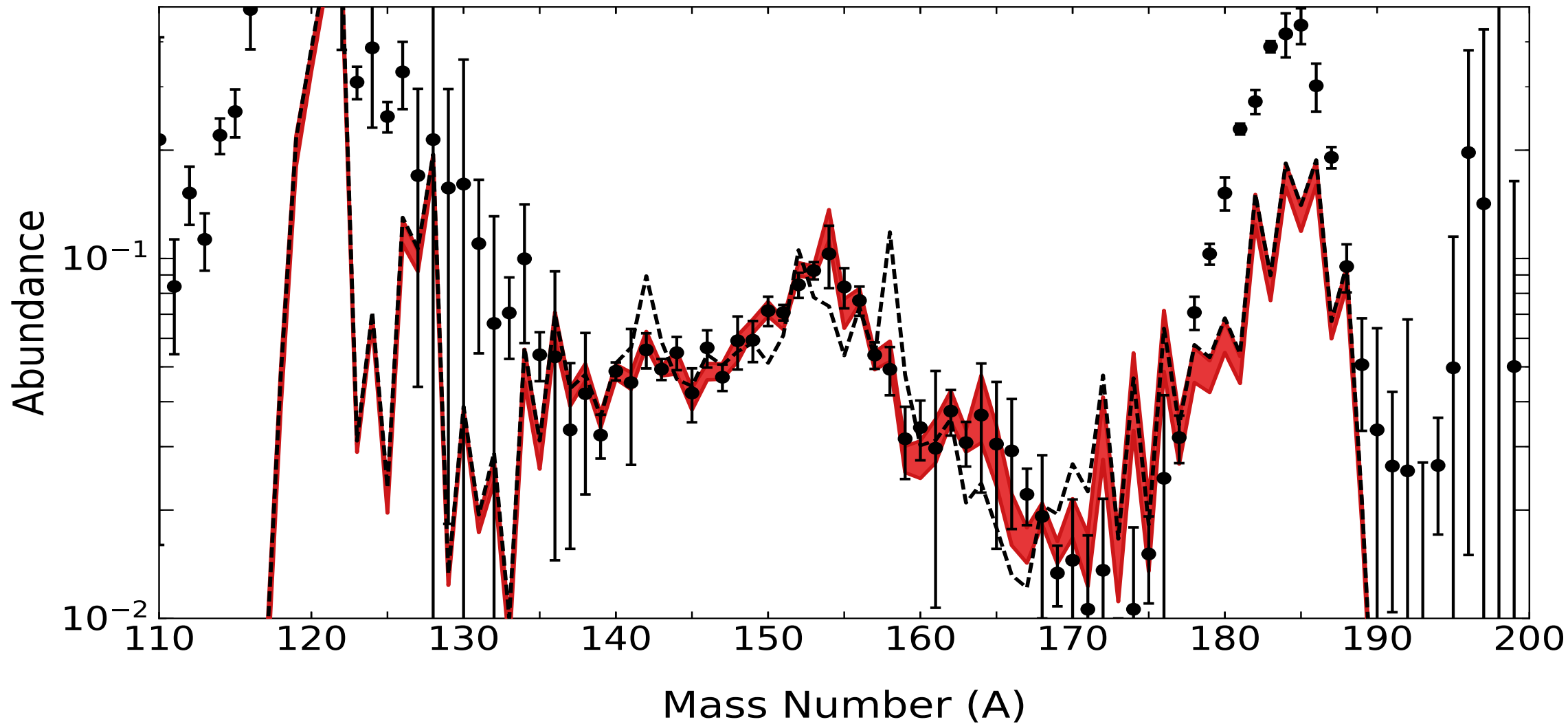
Goriely (2015)

Peak Formation with an MCMC Mass Solution



Peak Formation with an MCMC Mass Solution





(Abundance pattern range using the mass values found by our MCMC given disk wind conditions $s/k=30$, $\tau=70$ ms, $Y_e=0.2$)

Vassh et al (in preparation)

Measured Decay Rates and Masses

NUBASE 2016

β -decay, α -decay, and spontaneous fission

AME 2016 / Jyväskylä / CPT at CARIBU

